Primordial heavy noble gases in the pristine Paris carbonaceous chondrite

David V Bekaert, Yves Marrocchi, Alex Meshik, Laurent Remusat, Bernard Marty

The Meteoritical Society

Meteoritics & Planetary Science 54, Nr 2, 395–414 (2019)
doi: 10.1111/maps.13213

Primordial heavy noble gases in the pristine Paris carbonaceous chondrite

David V. BEKAERT[1*], Yves MARROCCHI[1], Alex MESHIK[2], Laurent REMUSAT[3], and Bernard MARTY[1]

[1]Centre de Recherches Pétrographiques et Géochimiques, CRPG-CNRS, Université de Lorraine, UMR 7358, 15 rue Notre Dame des Pauvres, BP 20, 54501 Vandoeuvre-lès-Nancy, France
[2]Department of Physics, Washington University, 1 Brookings Drive, Saint Louis, Missouri 63130, USA
[3]Institut de Minéralogie, de Physique des Matériaux et de Cosmochimie (IMPMC), UMR CNRS 7590 - Sorbonne, Universités - UPMC - IRD - Museum National d'Histoire Naturelle, 57 rue Cuvier, Case 52, 75231 Paris Cedex 5, France
[*]Corresponding author. E-mail: dbekaert@crpg.cnrs-nancy.fr

(Received 22 February 2018; revision accepted 08 October 2018)

Abstract–The Paris carbonaceous chondrite represents the most pristine carbonaceous chondrite, providing a unique opportunity to investigate the composition of early solar system materials prior to the onset of significant aqueous alteration. A dual origin (namely from the inner and outer solar system) has been demonstrated for water in the Paris meteorite parent body (Piani et al. 2018). Here, we aim to evaluate the contribution of outer solar system (cometary-like) water ice to the inner solar system water ice using Xe isotopes. We report Ar, Kr, and high-precision Xe isotopic measurements within bulk CM 2.9 and CM 2.7 fragments, as well as Ne, Ar, Kr, and Xe isotope compositions of the insoluble organic matter (IOM). Noble gas signatures are similar to chondritic phase Q with no evidence for a cometary-like Xe component. Small excesses in the heavy Xe isotopes relative to phase Q within bulk samples are attributed to contributions from presolar materials. CM 2.7 fragments have lower Ar/Xe relative to more pristine CM 2.9 fragments, with no systematic difference in Xe contents. We conclude that Kr and Xe were little affected by aqueous alteration, in agreement with (1) minor degrees of alteration and (2) no significant differences in the chemical signature of organic matter in CM 2.7 and CM 2.9 areas (Vinogradoff et al. 2017). Xenon contents in the IOM are larger than previously published data of Xe in chondritic IOM, in line with the Xe component in Paris being pristine and preserved from Xe loss during aqueous alteration/thermal metamorphism.

INTRODUCTION

Xenon isotopes have unique and resolvable isotopic signatures within different cosmological reservoirs of the solar system and, therefore, they constitute a powerful tool to decipher the contribution of planetary precursors (solar, chondritic, and cometary) to terrestrial planets and yield insights into the physical processes that affected planetary bodies over geological periods of time (Marty et al. 2017). While cometary materials constitute a pristine reservoir of the outer solar system building blocks, primitive meteorites (hereafter chondrites) are the only remnants of the inner solar system starting material. They consist of composite assemblages of high-temperature products from the protoplanetary disk phase (i.e., refractory inclusions, chondrules, Fe-Ni metal spherules) embedded in a volatile-rich and fine-grained matrix comprised of minerals, sulfides, and organic materials (Scott and Krot 2005). Volatile elements accreted at the time of asteroid formation may provide key information about the dynamics and physicochemical conditions of the accretionary disk where the building blocks of planetesimals formed and evolved. However, variable degrees of fluid alteration observed in the matrix of chondrites indicates that significant episodes of asteroidal alteration modified the chemistry of carbonaceous asteroids and probably affected the volatile element component inherited from this period of accretion (Palguta et al. 2010). Fluid circulations within asteroids likely arose from the melting of a

heterogeneously accreted water ice component, upon heating from the decay of extinct ^{26}Al and/or impact shocks.

The origin(s) and abundance of water accreted by carbonaceous asteroids remain(s) underconstrained (Brearley [2006] and references therein). Today, the innermost terrestrial planets contain little water relative to outer solar system planetary bodies. In the protoplanetary disk, the distribution of water ice was determined by the location of the snowline, i.e., the inner boundary of the region where the temperature is low enough for water to condense (Lecar et al. 2006). The position of the snow line is thought to have evolved through time—mostly inward, up to ~1 AU—as a function of the stellar accretion rate (Bitsch et al. 2015). The low water/rock ratios estimated from the O-isotopic characteristics of secondary minerals in carbonaceous chondrites suggest that carbonaceous asteroids formed close to the snowline, and not at greater heliocentric distances (Marrocchi et al. 2018).

Two principal sources are commonly considered regarding the origin of water ices in the region(s) of carbonaceous asteroid accretion: a locally derived water, directly condensed from the gas in the inner solar system (Alexander et al. 2012), and/or an outer disk water component inherited from the inward drift of outer solar system ices (Lunine 2006). Due to the self-shielding of ^{16}O-rich nebular CO gas by stellar UV light, the outer solar system component is ^{17,18}O-rich relative to inner solar system values (Lyons and Young 2005). It is also D-rich relative to the solar composition, possibly related to low-temperature ion-derived chemistry within the parent molecular cloud (Cleeves et al. 2014), although other scenarios such as gas-grain reactions, gas phase unimolecular photodissociation, and ultraviolet photolysis in D-enriched ice mantles have been advocated (Sandford et al. 2001). The respective proportions of local and outer solar system water ices accreted by carbonaceous asteroids are debated. Quantitative estimates of the contribution of "interstellar" ice to the inner solar system have been proposed from the analysis of hydrogen isotope ratios in the unequilibrated ordinary chondrite LL3.0 Semarkona (Piani et al. 2015) and in the pristine Paris meteorite (Vacher et al. 2016). The latter represents the least altered CM described to date (Hewins et al. 2014; Marrocchi et al. 2014; Rubin 2015). It has undergone variable degrees of alteration with moderately altered zones (CM 2.7) in direct contact with relatively fresh zones (CM 2.9) rich in Fe-Ni metal and pristine matrix (Hewins et al. 2014; Leroux et al. 2015). Such association suggests that some parts of the meteorite have been relatively preserved from the contribution of secondary fluid alteration. A schematic view of the heterogeneous accretion of the inner water ice component

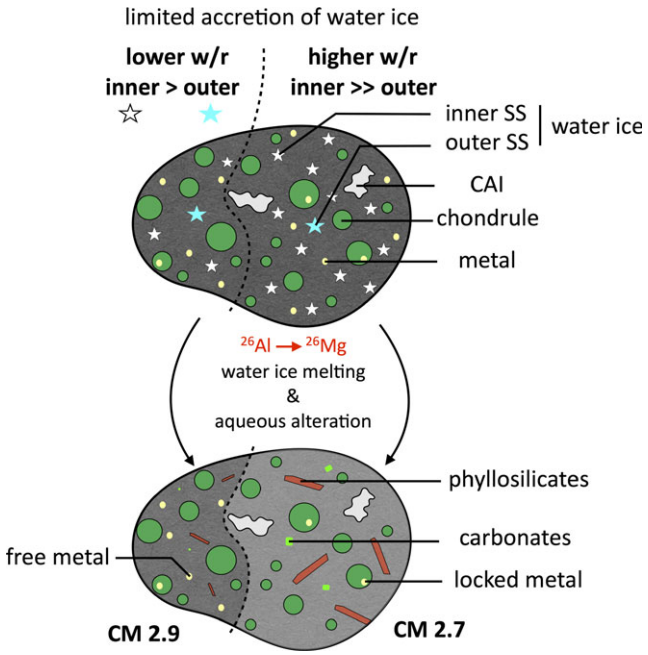

Fig. 1. A scenario for the Paris meteorite alteration history at the millimeter scale: the Paris meteorite parent body experienced a heterogeneous accretion of inner and outer solar system materials, with a limited amount of total water ice relative to other CM chondrites (Vacher et al. 2016; Piani et al. 2018). The subsequent melting of water ice induced an episode of heterogeneous aqueous alteration resulting in variable degrees of alteration with moderately altered zones (CM 2.7) in contact with relatively fresh zones (CM 2.9). The more altered (CM 2.7) zones are marked by the presence of numerous carbonates and phyllosilicates in the matrix (Fig. S1A in supporting information). These minerals are less abundant in the pristine (CM 2.9) areas, where free Fe-Ni metal is still observed (Rubin et al. 2007) (Fig. S1A). In CM 2.7 zones, Fe-Ni metal is only observed in chondrules. (Color figure can be viewed at wileyonlinelibrary.com.)

—as expected to have occurred on the Paris meteorite parent body—and related degrees of subsequent alteration is provided in Fig. 1.

The Paris meteorite exhibits enrichment in its bulk δD compared to the mean value of CM chondrites (120 ± 1‰ versus −69 ± 19‰, respectively; Vacher et al. 2016, 2017). In addition, the oxygen isotope signatures in carbonates of the Paris meteorite require the mixing of 8–35% of outer disk water with the CM local fluid from which some of the ^{17,18}O-rich Ca-carbonates precipitated (Vacher et al. 2016). This is consistent with the specific in situ C/H versus D/H correlation observed for the matrix of the Paris meteorite (Piani et al. 2018), suggesting the occurrence of D-rich fluids relative to other CM chondrites and, as such, a dual origin for the icy grains accreted by the parent body. Quantitative estimates of the contribution of outer solar system ice to the inner solar system have crucial implications regarding the extent of the radial mixing in the protoplanetary disk (Vacher et al. 2016) as well as the

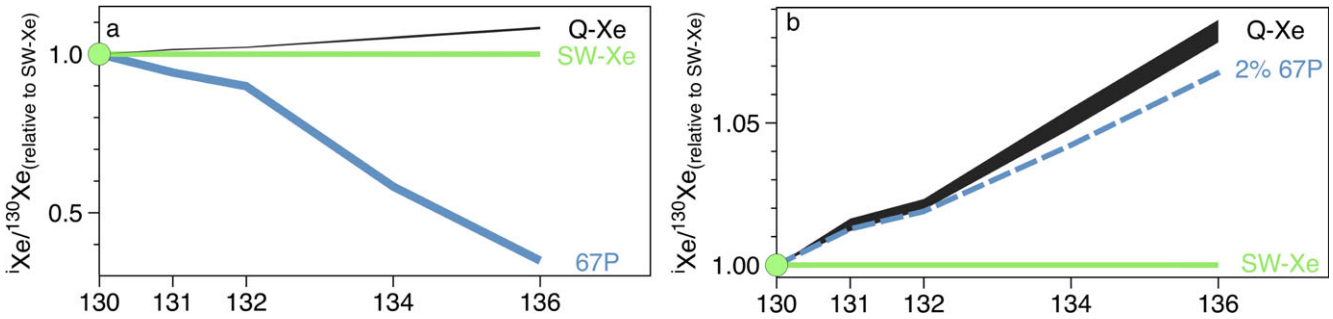

Fig. 2. a) Xenon isotopic spectra of the Q-phase (Busemann et al. 2000) and outer solar system (cometary-like; Marty et al. 2017) water ice, normalized to the solar composition (Meshik et al. 2014), showing that the Q-phase and cometary ice components have extremely different signatures for the heavy Xe isotopes. b) Magnified view of the Q-phase signature (Busemann et al. 2000) normalized to the solar composition (Meshik et al. 2014). We show that a 2% contribution of cometary ice to the total budget of Xe (with therefore 98% of Xe being of phase Q composition) would result in a measurable shift of the phase Q signature (dashed line). (Color figure can be viewed at wileyonlinelibrary.com.)

origin of the water accreted by asteroids and terrestrial planets (Drake 2005). However, the dichotomy between O and H isotope composition of water in the inner and outer solar system suggests low influx of D- and ^{17,18}O-rich water ice grains from the outer part of the solar system, possibly accounted for by the presence of a Jupiter-induced gap that limited the inward drift of outer solar system material into inner parts of the protoplanetary disk (Marrocchi et al. 2018).

The occurrence of outer solar system water signatures in the Paris meteorite (Piani et al. 2018) suggests that its parent body accreted cometary-like materials, likely including cometary ice, organic materials, and silicates. Cometary ice contains abundant Kr and Xe isotopes whose nucleosynthetic signatures are distinct from any known reservoir within the inner solar system (Rubin et al. 2018). Recently, the very first measurement of the Xe isotopic composition of Comet Churyumov–Gerasimenko (here 67P/C-G) by the ROSINA mass spectrometer on-board the Rosetta spacecraft revealed a new and unique composition characterized by strong $^{134–136}$Xe deficits relative to the solar composition (Marty et al. 2017) (Fig. 2). This outer solar system signature allowed the origin of Xe isotopes in the terrestrial atmosphere to be deciphered (Marty et al. 2017) and led to the suggestion that remnants of cometary noble gases may be preserved at the present-day lunar surface (Bekaert et al. 2017). Cometary bodies appear to be extremely rich in noble gases, so limited contributions of comets to planetary bodies have the potential to drastically affect the noble gas budget of planetary atmospheres (Marty et al. 2017). Thus, isotopes of xenon may provide a means to track contributions of outer solar system (cometary-like) material to the inner solar system (chondritic-like) planetary bodies. They therefore constitute a promising tool to investigate the dual origin of the icy grains (with outer and inner solar system signatures, respectively) accreted by the parent body of the Paris meteorite. These two water ice components most likely coexisted on the parent asteroid at the time of its accretion and were not mixed together during melting and aqueous alteration (if physically isolated within the rock for example). Indeed, it is likely that ice accretion was spatially heterogeneous, as observed by the heterogeneous distribution of alteration phases in the matrix of chondrites (Le Guillou and Brearley 2014). In addition, aqueous alteration onto asteroidal parent bodies of meteorites mainly took place within geochemical microenvironments that were not connected together (Le Guillou and Brearley 2014; Pignatelli et al. 2016). This is due to the low permeability of chondrites (Bland et al. 2009), which precludes mixing between water components of different origin.

Cometary ice is extremely rich in noble gases (Rubin et al. 2018). During ice melting and subsequent aqueous alteration of the parent body, cometary noble gases may simply be lost to space, trapped within weathering products, or adsorbed onto the surface of organic materials present on the parent body, with limited isotopic fractionation (Marrocchi and Marty 2013). Alternatively, cometary noble gases might have been delivered to the meteorite parent body by isotopically distinct cometary insoluble organic matter (Fray et al. 2016), silicates, and/or presolar grains. If present in the Paris meteorite, cometary noble gases may therefore be locked in the IOM, in addition to the common chondritic IOM carrying the ubiquitous phase Q component (Busemann et al. 2000), or spread out within the bulk sample. The phase Q component is enriched in heavy elements and heavy isotopes compared to the solar wind composition (Busemann et al. 2000) (Fig. 2). Q-Xe and Q-Kr are thus enriched by ~1% u^{-1} in their heavy isotopes relative to solar Xe. Additions of nucleosynthetic components such as Xe-HL (a combination of Xe-H, which is enriched in the heavy isotopes, and Xe-L, enriched in light xenon isotopes

(Reynolds and Turner 1964; Lewis et al. 1987) are required for mass-dependently fractionated solar Xe to adequately fit Q-Xe. The association of Xe-Q with Xe-HL has been suggested by Lavielle and Marti (1992), Marti and Mathew (1998), and Busemann et al. (2000). Using solar Xe composition found in lunar regolith, Gilmour (2010) estimated the contribution of ^{132}Xe-HL to be 1.5%. Meshik et al. (2014) used solar wind Xe composition measured in Genesis return samples and calculated 1.6% ^{132}Xe-HL contribution to slightly fractionated solar wind. Crowther and Gilmour (2013) estimated the same contribution of Xe-HL using a slightly modified solar wind composition. The exact host phase of the Q-gases in chondrites is not well characterized but appears to be intimately linked with refractory organic compounds (Ott et al. 1981; Busemann et al. 2000; Marrocchi et al. 2011; Kuga et al. 2015). As depicted in Fig. 2, even a minor contribution of 2% cometary-like Xe (calculated based on ^{132}Xe and using the composition of comet 67P/C-G; Marty et al. 2017) to phase Q xenon would result in a noticeable and detectable shift of the heavy isotope ratios toward lower values. Analyzing separately the heavy noble gas isotopic composition of the IOM and bulk fragments constitutes therefore a promising way to investigate the occurrence of cometary noble gases in the Paris meteorite.

In the present study, we analyzed the Paris meteorite for its argon, krypton, and xenon isotopes by discriminating mostly pristine (2.9 CM) and mostly altered (2.7 CM) fragments of the meteorite. We also analyzed separately the insoluble organic matter (IOM) chemically isolated from a bulk sample of the Paris meteorite for Ne (low precision), Ar, Kr, and Xe isotopes. Unlike Kr and Xe, which are dominated by the Q component in primitive meteorites, neon is expected to be dominated by a presolar component in the diamonds, the Ne-HL (Ott 2014). The possibility of tracing a possible contribution of cometary organic materials together with cometary water ice opens interesting perspectives since the isotopic signature of noble gases in cometary IOM is not known. Noble gas elemental fractionation during aqueous alteration may also provide information on the extent of secondary alteration on the parent body and on the nature of the phases bearing Q-gases (Browning et al. 1996; Weimer et al. 2017).

MATERIAL AND METHODS

Preparation of the Two CM 2.7 and Two CM 2.9 Fragments

A thin section of the Paris chondrite was polished on both sides and coated under vacuum with a thin layer of pure carbon to provide conductive surfaces. Both sides of the section were examined using a scanning electron microscope (SEM) (JEOL JSM-6510) equipped with an energy dispersive X-ray (EDX) Genesis detector (CRPG, Nancy), with a 3 nA electron beam accelerated at 15 kV. After observation, the sample was polished on both sides using a 0.25 μm diamond polishing powder in ethanol to remove any residue of the pure carbon layer.

As already described in previous works for other subsamples of the Paris meteorite (Marrocchi et al. 2014; Rubin 2015; Pignatelli et al. 2016, 2017; Vacher et al. 2016), our thin section presents variable degrees of alteration on both sides characterized by significant differences in the abundance of Fe-Ni metal beads. According to the alteration scale proposed by Rubin et al. (2007), the more altered zones are characterized by the presence of numerous carbonates and phyllosilicates in the matrix and were classified as CM 2.7 (Hewins et al. 2014; Marrocchi et al. 2014; Rubin 2015). These minerals are less abundant in the more pristine areas, marked by the presence of free Fe-Ni metal and classified as CM 2.9 (Fig. S1). In CM 2.7 zones, Fe-Ni metal is mainly observed when locked in chondrules. A pristine (2.9 CM) central area is observed on both sides of the thin section, suggesting that the central part of the sample is not altered, contrary to the surrounding mostly 2.7 CM material (Fig. S1). Four pieces of the sample (~5 mg each) were selected for noble gas analysis, from the central pristine area (fragments 4 and 5, Fig. S1) and from the more altered areas (fragments 2 and 8, Fig. S1).

The four pieces were separated using a diamond wire saw (0.3 mm Ø) at very low speed, in order to prevent heating, and avoiding the use of water as a lubricant to limit contamination of the sample. Droplets of pure ethanol were periodically deposited onto the saw to facilitate the removal of dust. The four pieces were then dried at 90 °C for 1 h, before being weighted and set into the CO_2 infrared (λ = 10.6 μm) laser extraction chamber (Humbert et al. 2000) under high vacuum (10^{-9} mbar) at 110 °C for 2 days. This preheating of the sample allowed weakly bound atmospheric gases to be degassed prior to noble gas analysis.

Noble Gas Isotopic Measurements (CM 2.7 and CM 2.9 Fragments)

Argon, krypton, and xenon were extracted by heating the samples with a CO_2 infrared (λ = 10.6 μm) laser (Humbert et al. 2000). In this method, the first extraction is typically carried out by slowly increasing the laser power until the heated sample turns reddish (sample's temperature being therefore qualitatively estimated to be ~600 °C, depending on the mineralogical composition of the sample [Bekaert et al. 2017]. Here, because part of the noble gas content of the sample may be already degassed at this temperature, we only performed a single (~10 min) step of sample melting at T > 1600 °C. The formation of a

spherule of molten silicate indicated that the melting temperature of the sample had been reached, and that more than 99% of the gas had been extracted (Humbert et al. 2000). A re-extraction was carried out on fragment 4, with negligible amounts of gas being released, in line with a complete extraction of the gas upon initial melting. However, note that Huss et al. (1996) observed significant gas release at temperatures >1800 °C. The possibility to have preserved some noble gases, especially Kr and Xe, in very refractory phases of these bulk fragments cannot be excluded. If that fraction of the sample gas were to be only extracted at temperatures >1800 °C, it could not be analyzed in the present experimental setting. Series of standards were run between each sample each day for subsequent spectrometer mass discrimination corrections. Blanks accounted for <0.5% of the ^{36}Ar, ^{84}Kr, and ^{130}Xe released from the samples, making blank correction negligible. Extracted gases were purified using two Ti-sponge getters held at 650 °C for 5 min and then cooled down to room temperature over the next 5 min. Xenon and krypton were separated from Ar on the surface of a Pyrex finger held at liquid nitrogen temperature for 20 min. Argon isotopic measurements were first carried out on the remaining fraction with a Helix MC Plus (Thermofisher Scientific) mass spectrometer. The partial pressure of Ar in the volume of the glass finger was then reduced by diluting five times the volume trapped in the cold finger, still at liquid nitrogen temperature, into the whole line set under static vacuum. The Pyrex finger held at liquid nitrogen temperature was then isolated from the line during pumping. Finally, the Pyrex finger (containing the Xe and Kr) was warmed to room temperature and the gases released were exposed once again to two further hot Ti-sponge getters for final purification. The line was then divided into 3–6 sections of approximately equal volumes to carry out repeated analyses of Xe and Kr isotopes, with Xe isotopes being systematically analyzed first. Krypton and xenon isotopes were measured with a Helix MC Plus (Thermofisher Scientific) mass spectrometer by peak jumping on the central compact dynode electron multiplier AX (Compact Discrete Dynode).

Preparation of the Insoluble Organic Residue

A matrix-enriched subsample (~8 g) of the Paris meteorite (unknown lithology, CM 2.7, CM 2.9, or a mixture of the two) was crushed in an agate mortar before isolating IOM using the protocols described by Remusat et al. (2005, 2008) and Vinogradoff et al. (2017). In summary, the powdered matrix was subjected to several extractions in water (stirring under reflux for 48 h), acetone (stirring at room temperature for 2 h, twice), and dichloromethane/methanol (2:1, vol/vol, stirring at room temperature for 2 h, twice). The solid residue was then subjected three times to HF/HCl treatment by stirring successively in a mixture of HF/HCl (16 N/2 N, 2:1, vol/vol) for 24 h at room temperature under nitrogen flux. The residue was then washed several times with HCl (6 N) for 2 h at 70 °C (i.e., to remove fluoride compounds) until the final solute was colorless. The acid residue was then washed with bidistilled water until neutrality, extracted three times with acetone and a mixture of CH_2Cl_2/MeOH, 2:1 vol/vol and subsequently dried under nitrogen. A residue of about 150 mg (i.e., ~1.8 wt% of the initial sample) was recovered at the end of this procedure. Some 0.44 mg of this residue was analyzed for its noble gas content and isotopic composition by stepped pyrolysis.

Noble Gas Isotopic Measurements (IOM)

The Paris meteorite IOM (0.44 mg) was wrapped in platinum foil and then loaded into a glass sample tree. The samples were gently baked in vacuum at 150 °C for 3 days in order to remove adsorbed atmospheric gases. Noble gases were extracted by stepped pyrolysis in the temperature range 300–1768 °C using a tungsten coil. The linear current–temperature calibration curve for the coil was obtained using an optical pyrometer with a precision of ±25 °C for temperatures above 800 °C. The calibration curve was extrapolated to temperatures lower than 800 °C. Gas extraction from the IOM was thus carried out by stepwise heating at 570, 790, 980, 1225, 1539, and 1770 °C. Extraction times were adjusted as a function of temperature, i.e., (1) 15 min for the four low-temperature steps (i.e., 300–1300 °C), (2) 12 min for the 1539 °C step, and (3) 5 min for the final step (at the platinum melting point: 1770 °C). The released gases were exposed to three consecutive pellet getters containing SAES St172 getter alloy in order to remove active gases (10 min at 275 °C and 10 min at room temperature). Argon, krypton, and xenon were held on a charcoal finger at liquid nitrogen temperature for 45 min, then the residual light noble gases were analyzed for their Ne isotopes. Active charcoal immersed into liquid nitrogen was then heated to −105 °C using an external heater that surrounds the charcoal. The temperature was regulated within ±1 °C by PID controller. Calibration curves determined from air standards showed that Kr and Xe are not affected at this temperature while ~70% of the Ar is released. This procedure reduces the amount of Ar in the mass spectrometer, which has a considerable effect on the mass discrimination of krypton and xenon. Argon released from the charcoal finger was then pumped out for 5 min. The liquid nitrogen was then removed, and the charcoal finger was heated to 160 °C for 25 min to

Table 1. Neon abundances and isotopic compositions of the Paris meteorite IOM via stepwise heating. The total amount of extracted ^{20}Ne is given via the abundance-weighted mean isotopic composition.

T°C	^{20}Ne (cm^3 STP/g)	±2σ	^{21}Ne/^{22}Ne	±2σ	^{20}Ne/^{22}Ne	±2σ
572	6.14E-08	9.39E-09	0.0331	0.0047	10.5795	1.4331
790	1.95E-07	2.38E-08	0.0307	0.0016	9.4681	0.4463
980	7.71E-07	1.00E-07	0.0313	0.0006	8.7100	0.1156
1225	4.90E-07	6.42E-08	0.0338	0.0008	9.0149	0.1803
1539	1.28E-07	1.69E-08	0.0359	0.0028	10.2103	0.7385
1770	6.65E-08	9.44E-09	0.0353	0.0051	11.7341	1.6663
Total	1.71E-06	2.24E-07	0.0325	0.0012	9.1804	0.3258

Table 2. Argon abundances and isotopic compositions of the Paris meteorite IOM via stepwise heating. The total amount of extracted ^{36}Ar is given via the abundance-weighted mean ^{38}Ar/^{36}Ar.

T°C	^{36}Ar (cm^3 STP/g)	±2σ	^{38}Ar/^{36}Ar	±2σ
408	3.18E-09	1.11E-09	0.2087	0.0022
572	1.35E-07	2.09E-08	0.2613	0.0019
790	1.14E-06	1.37E-07	0.2035	0.0008
980	1.58E-06	2.02E-07	0.1932	0.0006
1225	2.92E-06	3.91E-07	0.1904	0.0002
1539	3.08E-07	4.07E-08	0.2003	0.0013
1770	6.48E-07	9.07E-08	0.1973	0.0004
Total	6.73E-06	8.84E-07	0.1958	0.0005

release Xe, Kr, and the residual fraction of Ar. Heavy noble gases were then introduced into high-sensitivity (~5×10^{-16} cm^{3}STP/Hz for Kr) mass spectrometer equipped with Baur–Signer ion source (Washington University, Saint Louis, USA) (Mabry et al. 2007; Meshik et al. 2007) for determination of Ar, Kr, and Xe abundances and ^{38}Ar/^{36}Ar, ^{86}Kr/^{84}Kr, and ^{129}Xe/^{132}Xe isotopic ratios. Blanks were measured for each extraction temperature and used to correct the data. Hot blanks (1200 °C) were also performed several times during each analytical session. The Kr and Xe concentrations within Pt foils were also measured and appeared to be negligible. The uncertainties in isotopic ratios (2σ) include hot blank, standard, and internal (statistical and internal mass fractionation) error propagation. Note that Kr extracted at 1539 °C was accidentally pumped and so no Kr data could be obtained for this temperature step.

RESULTS

All data are reported in Tables 1–7. Neon, argon, krypton, and xenon isotopic data for the IOM are reported in Tables 1, 2, 4, and 6, respectively. Noble gas isotopic data for the bulk fragments are reported in Tables 3, 5, and 7, respectively.

Argon, krypton, and xenon isotope compositions of the pristine CM 2.9 fragments, the CM 2.7 fragments, and the bulk IOM of the Paris meteorite are dominated by the Q component (Figs. 3 and 4). In agreement with Hewins et al. (2014), we consistently measured very low ^{40}Ar/^{36}Ar ratios (~3, while the atmospheric ratio is 298.56 ± 0.31; Lee et al. 2006) for the bulk CM 2.7 and CM 2.9 fragments (Table 3). Although Kr isotope compositions are similar to phase Q-Kr in CM 2.7 and CM 2.9 fragments (Fig. 3a), Xe isotopes show excesses in the heavy isotopes relative to Q-Xe (Fig. 4a). The ^{136}Xe/^{130}Xe excesses are ~2% relative to Q-Xe. Importantly, no difference could be detected between the noble gas isotope composition of the CM 2.9 and CM 2.7 fragments (Figs. 3 and 4). Likewise, no obvious difference in Kr (~1.4×10^{-8} cm^3 STP ^{84}Kr/g) and Xe (~1.7×10^{-8} cm^3 STP ^{132}Xe/g) contents between CM 2.9 and CM 2.7 fragments of the Paris meteorite is observed (Tables 5 and 7). However, argon appears to be slightly depleted in the CM 2.7 (~1.49×10^{-6} cm^3 STP ^{36}Ar/g) relative to CM 2.9 (~1.86×10^{-6} cm^3 STP ^{36}Ar/g) fragments (Table 3). A second extraction step on fragment 4 released ≤1% of the total amounts of its noble gas contents (Table 3, 5, and 7), in agreement with the fact that more than 99% of noble gases are extracted by CO_2 infrared laser heating when a spherule of molten silicate is obtained (Humbert et al. 2000).

In total, we found that 1.71×10^{-6} cm^3 STP ^{20}Ne, 6.73×10^{-6} cm^3 STP ^{36}Ar, 3.48×10^{-7} cm^3 STP ^{84}Kr, and 4.92×10^{-7} cm^3 STP ^{132}Xe were extracted from the Paris meteorite IOM over stepwise heating per gram of residue. Based on Ar and Kr release patterns, we estimate that the Kr missing step at 1539 °C would contribute <5% of the total amount of ^{84}Kr extracted from the IOM. Krypton and xenon are released altogether during the 1225 °C extraction step (>85% of ^{84}Kr and ^{132}Xe), in contrast to Ne and Ar, which are progressively released from 570 °C to 980 °C (Fig. S2 in supporting information). The peak release for neon is ~980°C. The abundance-weighted mean isotopic composition of the Paris meteorite IOM is consistent with a mixture of HL-Ne (Huss and Lewis 1994) and

Table 3. Argon abundances and isotopic compositions of the Paris meteorite CM 2.7 and CM 2.9 bulk fragments.

Sample	Mass (mg)	PT (CM)	^{36}Ar (cm^3 STP/g)	±2σ	^{38}Ar/^{36}Ar	±2σ	^{40}Ar/^{36}Ar	±2σ
Paris 2	2.42	2.7	1.48E-06	8.88E-08	0.2559	0.0018	4.3412	0.0286
Paris 8	3.50	2.7	1.50E-06	9.00E-08	0.1883	0.0008	2.6805	0.0467
Second extraction			3.34E-09	2.49E-09	0.2135	0.0090	3.3195	1.8124
Paris 4	6.54	2.9	1.87E-06	1.12E-07	0.1880	0.0005	2.9992	0.0432
Paris 5	2.98	2.9	1.85E-06	1.11E-07	0.1985	0.0009	2.5578	0.0370

PT = petrologic type.

Table 4. Krypton abundances and isotopic compositions of the Paris meteorite IOM via stepwise heating. The total amount of extracted ^{84}Kr is given via the abundance-weighted mean isotopic composition.

T°C	^{84}Kr (cm^3 STP/g)	±2σ	^{80}Kr/^{84}Kr	±2σ	^{82}Kr/^{84}Kr	±2σ	^{83}Kr/^{84}Kr	±2σ	^{86}Kr/^{84}Kr	±2σ
572	7.84E-09	1.22E-09	0.0392	0.0005	0.2023	0.0019	0.2026	0.0017	0.3079	0.0024
790	1.16E-08	1.83E-09	0.0393	0.0005	0.2020	0.0015	0.2027	0.0012	0.3104	0.0016
980	9.69E-09	1.28E-09	0.0387	0.0008	0.2003	0.0019	0.2025	0.0021	0.3077	0.0018
1225	3.02E-07	4.05E-08	0.0394	0.0006	0.2009	0.0014	0.2013	0.0014	0.3095	0.0019
1539	–	–	–	–	–	–	–	–	–	–
1770	1.67E-08	2.35E-09	0.0392	0.0004	0.2026	0.0011	0.2028	0.0013	0.3085	0.0017
Total	3.48E-07	4.72E-08	0.0394	0.0006	0.2010	0.0014	0.2015	0.0014	0.3094	0.0019

Q-Ne (Busemann et al. 2000) with possible small additions of cosmogenic Ne released during the highest temperature steps (Fig. 5). Xenon heavy isotope excesses relative to Q-Xe, similar to those reported for bulk CM 2.7 and CM 2.9 fragments, are also observed in the IOM for the 980 °C, 1225 °C, and (to a small extent) 1539 °C extraction steps (Fig. 4b). The abundance-weighted mean isotopic composition of the Paris meteorite IOM is similar to that of Q-Xe, with slight relative excesses in the heavy isotopes (Fig. 6). From a simple mass balance, we find that the Paris meteorite's IOM, which constitutes <2 wt% of the bulk sample (see the Preparation of the Insoluble Organic Residue section), contains more than 50% of the total amount of Xe present in the meteorite. The remaining Xe might reside within the soluble fraction of organic matter (removed during IOM isolation) or within mineral phases (removed during the HF/HCl treatment).

DISCUSSION

Noble Gas Signatures of the Paris Meteorite

In agreement with Hewins et al. (2014), we found the Xe signature of the Paris meteorite to be dominated by a Q-like component, as is often the case for carbonaceous chondrites (Busemann et al. 2000). Note, however, that the Xe isotopic spectrum reported by Hewins et al. (2014) for the Paris meteorite exhibits an anomalously high ^{126}Xe/^{130}Xe that we attribute to an analytical issue (Fig. 6). From the high-precision measurements conducted in this study, we confirm that the Q component dominates the Xe isotope signature of the Paris meteorite. As explained by Hewins et al. (2014), ^{38}Ar cosmogenic ages of the sample could not be determined as the argon content of Paris is dominated by the Q component, precluding a good estimate of the abundance of cosmogenic ^{38}Ar. The very low ^{40}Ar/^{36}Ar ratio (~3; Table 3) indicates limited contamination by atmospheric and radiogenic argon. Our data show no difference between CM 2.7 and CM 2.9 fragments for the Xe isotope composition, with both series of data comprising excesses in the heavy isotopes ($^{132–136}$Xe) relative to Q-Xe (Fig. 4a).

The Xe isotope composition of comets appears to be nucleosynthetically distinct from solar or Q signatures (Marty et al. 2017), which are related by mass-dependent fractionation. Cometary Xe is identical to solar Xe with the exception of the two heaviest isotopes, ^{134}Xe and ^{136}Xe. Thus, a possibility is that the solar/Q nucleosynthetic reservoir was derived from a cometary-like nucleosynthetic reservoir by addition of a nucleosynthetic component with excesses in the heavy Xe isotopes. Such a component (labeled Xe-H) has long been detected in primitive chondrites, always associated with an additional component showing overabundance of the light Xe isotopes (Xe-L) (Reynolds and Turner 1964). Xe-H and Xe-L were probably formed by different nucleosynthetic processes and the ultimate splitting of the heavy and light isotope subcomponents of Xe-HL, which have long been considered inseparable, may be achievable although no solid evidence has been found yet (Meshik et al. 2001). Gilmour and Turner (2007) demonstrated such a possibility using theoretical constraints to three-dimensional fits of xenon isotope data from presolar grains. These two components would notably be required

Table 5. Krypton abundances and isotopic compositions of the Paris meteorite CM 2.7 and CM 2.9 bulk fragments.

Sample	Mass (mg)	PT (CM)	^{84}Kr (cm^3 STP/g)	±2σ	^{80}Kr/^{84}Kr	±2σ	^{82}Kr/^{84}Kr	±2σ	^{83}Kr/^{84}Kr	±2σ	^{86}Kr/^{84}Kr	±2σ
Paris 2	2.42	2.7	1.33E-08	6.31E-10	0.0393	0.0013	0.2029	0.0044	0.2019	0.0049	0.3091	0.0067
			1.37E-08	6.84E-10	0.0397	0.0017	0.2024	0.0042	0.2025	0.0037	0.3091	0.0059
			1.44E-08	7.64E-10	0.0395	0.0014	0.2014	0.0054	0.2011	0.0067	0.3079	0.0079
		Average	1.38E-08	7.78E-10	0.0395	0.0003	0.2022	0.0010	0.2018	0.0010	0.3087	0.0010
Paris 8	3.50	2.7	1.25E-08	5.90E-10	0.0395	0.0012	0.2022	0.0038	0.2017	0.0046	0.3085	0.0057
			1.28E-08	6.12E-10	0.0396	0.0014	0.2015	0.0047	0.2030	0.0046	0.3100	0.0066
			1.27E-08	6.23E-10	0.0391	0.0015	0.2025	0.0048	0.2011	0.0049	0.3099	0.0077
		Average	1.27E-08	5.49E-10	0.0394	0.0003	0.2021	0.0007	0.2019	0.0014	0.3094	0.0012
Second extraction			7.86E-10	7.31E-11	0.0419	0.0062	0.2087	0.0279	0.2061	0.0339	0.3040	0.0303
Paris 4	6.54	2.9	1.35E-08	6.85E-10	0.0395	0.0012	0.2021	0.0050	0.2019	0.0047	0.3073	0.0071
			1.33E-08	6.47E-10	0.0393	0.0010	0.2009	0.0052	0.2025	0.0050	0.3082	0.0053
			1.30E-08	5.99E-10	0.0398	0.0014	0.2018	0.0044	0.2029	0.0040	0.3103	0.0053
			1.40E-08	7.17E-10	0.0395	0.0012	0.2028	0.0039	0.2025	0.0044	0.3093	0.0055
		Average	1.38E-08	7.65E-10	0.0396	0.0002	0.2019	0.0009	0.2024	0.0005	0.3088	0.0015
Paris 5	2.98	2.9	1.37E-08	7.10E-10	0.0395	0.0015	0.2015	0.0042	0.2019	0.0044	0.3103	0.0046
			1.43E-08	6.79E-10	0.0397	0.0016	0.2028	0.0046	0.2022	0.0042	0.3090	0.0057
			1.50E-08	8.54E-10	0.0396	0.0016	0.2013	0.0049	0.2017	0.0055	0.3091	0.0058
		Average	1.43E-08	7.58E-10	0.0396	0.0002	0.2019	0.0011	0.2019	0.0003	0.3095	0.0010

PT = petrologic type.

to be separated with extra Xe-H being added to solar, without any addition of Xe-L (Ott 2014). However, the Xe-H and Xe-L components always occur together at a constant abundance ratio (the so-called Xe-HL component), carried together in presolar nanodiamonds (Lewis et al. 1987). Gilmour et al. (2005) argued that the lack of variation in the Xe-HL component might also be a direct consequence of its definition, a different name (e.g., P3, P6) being given to any enrichment showing a different H/L ratio.

When the Xe-Q isotope composition is normalized to SW-Xe and corrected for mass-dependent fractionation, excesses in $^{134–136}$Xe are observed and are generally attributed to the contribution of a non-fissiogenic Xe component born by an unidentified carrier with the same Xe-HL isotopic composition as HL-bearing nanodiamonds (Gilmour 2010). Interestingly, Riebe et al. (2017) found that primordial Ne and Xe in the HF-solubles of the CI chondrite Ivuna also have isotopic and elemental ratios corresponding to a mixture of HL and Q. Xenon-134 and ^{136}Xe are produced only in the nucleosynthetic *r*-process (Ott 1996). While nanodiamonds are possibly unaffected by etching (Lewis et al. 1987), the exact Q-Xe composition (with the Xe-HL subcomponent, Huss and Lewis 1994) is observed by online nitric oxidation of acid residues (Busemann et al. 2000). Xe-HL host phases other than nanodiamonds have not yet been isolated (Gilmour 2010; Meshik et al. 2014) and additional Xe components (e.g., Xe-S carried by Si-C and graphite) may be required to account for the origin of the Q-Xe signature (Meshik et al. 2014). Here, we compute that a contribution of 1.8% of Xe-H to Q-Xe (calculated using the maximum $[^{131}Xe/^{136}Xe]_{Xe\text{-}H}$ given by Gilmour and Turner [2007] and the Q composition provided by Busemann et al. [2000]) can account for the $^{134–136}$Xe excesses relative to Q. This is in good agreement with previous estimates of the contribution of the Xe-HL component in carbonaceous chondrites (e.g., 1.5% Xe-HL for ^{132}Xe in Orgueil meteorite; Ott 2014). However, ^{126}Xe/^{132}Xe ratios, and their associated uncertainties, in the bulk fragments of the Paris meteorite preclude any additional contribution from Xe-L relative to the Q composition (Fig. 4a).

Excesses in the heavy isotopes ($^{132–136}$Xe) relative to Q-Xe, as observed in CM 2.7 and CM 2.9 fragments, can also be compared to the spectra of spontaneous fission of ^{238}U (dotted lines Fig. S3 in supporting information) and ^{244}Pu (dashed lines Fig. S3) (Porcelli and Ballentine 2002) that would be expected to account for the measured excesses in ^{136}Xe. However, the excesses we detected relative to Q-Xe are all relatively minor such that the $^{131–136}$Xe/^{130}Xe predicted from fission of ^{238}U and ^{244}Pu are all within error of the data points, thus preventing any accurate discrimination between a dominant contribution of ^{238}U- or ^{244}Pu-Xe (Fig. S3). The bulk U content of the Paris meteorite has been determined to be 1.01×10^{-2} μg/g (Hewins et al. 2014) (i.e., ~4.24×10^{-11} mol ^{238}U/g). By (1) using the product of the decay constant (λ_{sf}) and of the fractional yield of ^{136}Xe ($^{136}Y_{sf}$) produced by the spontaneous fission of ^{238}U ($[6.83 \pm 0.18] \times 10^{-18}$ a^{-1}; Ragettli et al. 1994) and (2) assuming a closure age of

Table 6. Xenon abundances and isotopic compositions of the Paris meteorite IOM via stepwise heating. The total amount of extracted ^{132}Xe is given via the abundance-weighted mean isotopic composition.

T°C	^{132}Xe (cm^3 STP/g)	±2σ	$^{124}Xe/^{132}Xe$	±2σ	$^{126}Xe/^{132}Xe$	±2σ	$^{128}Xe/^{132}Xe$	±2σ	$^{129}Xe/^{132}Xe$	±2σ	$^{130}Xe/^{132}Xe$	±2σ	$^{131}Xe/^{132}Xe$	±2σ	$^{134}Xe/^{132}Xe$	±2σ	$^{136}Xe/^{132}Xe$	±2σ
572	7.15E-09	1.12E-09	0.0045	0.0002	0.0040	0.0001	0.0822	0.0010	1.0467	0.0042	0.1627	0.0014	0.8231	0.0030	0.3753	0.0023	0.3153	0.0019
790	1.01E-08	1.56E-09	0.0045	0.0001	0.0040	0.0002	0.0828	0.0007	1.0343	0.0042	0.1628	0.0010	0.8198	0.0037	0.3756	0.0014	0.3153	0.0019
980	1.35E-08	1.82E-09	0.0046	0.0002	0.0041	0.0002	0.0830	0.0010	1.0365	0.0064	0.1622	0.0017	0.8193	0.0062	0.3839	0.0022	0.3244	0.0018
1225	4.26E-07	5.58E-08	0.0046	0.0001	0.0041	0.0001	0.0834	0.0006	1.0421	0.0042	0.1640	0.0011	0.8215	0.0029	0.3805	0.0010	0.3220	0.0016
1539	1.65E-08	2.38E-09	0.0045	0.0001	0.0040	0.0001	0.0828	0.0008	1.0407	0.0048	0.1624	0.0010	0.8200	0.0027	0.3784	0.0016	0.3183	0.0015
1770	1.90E-08	2.70E-09	0.0044	0.0001	0.0040	0.0001	0.0830	0.0005	1.0393	0.0044	0.1635	0.0008	0.8197	0.0026	0.3771	0.0016	0.3170	0.0012
Total	4.92E-07	6.54E-08	0.0046	0.0001	0.0041	0.0001	0.0833	0,0006	1.0417	0.0043	0.1638	0.0011	0.8213	0.0030	0.3802	0.0011	0.3215	0.0016

Table 7. Xenon abundances and isotopic compositions of the Paris meteorite CM 2.7 and CM 2.9 bulk fragments.

Sample	Mass (mg)	PT (CM)	^{132}Xe (cm^3 STP/g)	±2σ	^{124}Xe/^{132}Xe	±2σ	^{126}Xe/^{132}Xe	±2σ	^{128}Xe/^{132}Xe	±2σ	^{129}Xe/^{132}Xe	±2σ	^{130}Xe/^{132}Xe	±2σ	^{131}Xe/^{132}Xe	±2σ	^{134}Xe/^{132}Xe	±2σ	^{136}Xe/^{132}Xe	±2σ
Paris 2	2.42	2.7	1.85E-08	5.05E-10	0.00455	0.00032	0.00404	0.00037	0.08217	0.00280	1.03696	0.02681	0.16142	0.00275	0.81879	0.02407	0.38260	0.01071	0.32235	0.00869
			1.84E-08	5.46E-10	0.00461	0.00043	0.00400	0.00026	0.08160	0.00279	1.03848	0.02881	0.16231	0.00339	0.82077	0.02951	0.38349	0.01132	0.32346	0.00958
			1.96E-08	5.35E-10	0.00453	0.00022	0.00400	0.00021	0.08210	0.00299	1.04090	0.02091	0.16238	0.00278	0.81880	0.02420	0.38306	0.00812	0.32324	0.00622
	Average		1.88E-08	9.69E-10	0.00456	0.00006	0.00401	0.00004	0.08196	0.00044	1.03878	0.00281	0.16203	0.00075	0.81945	0.00161	0.38305	0.00063	0.32301	0.00083
Paris 8	3.50	2.7	1.64E-08	5.07E-10	0.00450	0.00034	0.00400	0.00028	0.08150	0.00252	1.03744	0.02818	0.16136	0.00300	0.81612	0.02628	0.38371	0.01093	0.32202	0.00965
			1.60E-08	4.82E-10	0.00460	0.00027	0.00400	0.00031	0.08171	0.00286	1.04006	0.02436	0.16196	0.00283	0.81815	0.02467	0.38301	0.00960	0.32249	0.00888
			1.61E-08	4.52E-10	0.00460	0.00036	0.00405	0.00037	0.08219	0.00270	1.03920	0.02064	0.16115	0.00219	0.81333	0.01925	0.38327	0.00960	0.32300	0.00813
	Average		1.62E-08	3.43E-10	0.00457	0.00008	0.00402	0.00004	0.08180	0.00050	1.03890	0.00189	0.16149	0.00060	0.81587	0.00342	0.38333	0.00050	0.32250	0.00069
Second extraction			1.27E-10	1.73E-11	0.00440	0.00173	0.00341	0.00156	0.07677	0.01880	1.01171	0.18563	0.15229	0.02037	0.79102	0.18915	0.38242	0.07601	0.31529	0.06146
Paris 4	6.54	2.9	1.60E-08	5.18E-10	0.00457	0.00041	0.00399	0.00042	0.08197	0.00304	1.03841	0.03003	0.16138	0.00339	0.81515	0.02970	0.38226	0.01078	0.32161	0.00994
			1.58E-08	4.48E-10	0.00458	0.00038	0.00402	0.00039	0.08182	0.00276	1.03578	0.02141	0.16158	0.00229	0.81321	0.02002	0.38068	0.00884	0.32250	0.00702
			1.53E-08	5.45E-10	0.00452	0.00043	0.00393	0.00044	0.08192	0.00366	1.03558	0.03832	0.16219	0.00420	0.81876	0.03662	0.38175	0.01594	0.32023	0.01177
			1.67E-08	4.58E-10	0.00451	0.00029	0.00400	0.00024	0.08171	0.00252	1.03334	0.01782	0.16115	0.00196	0.81588	0.01716	0.38129	0.00735	0.32143	0.00635
			1.70E-08	5.31E-10	0.00463	0.00025	0.00403	0.00036	0.08164	0.00271	1.04260	0.02896	0.16197	0.00312	0.81974	0.02726	0.38415	0.01032	0.32330	0.00962
			1.71E-08	5.33E-10	0.00462	0.00025	0.00403	0.00036	0.08184	0.00272	1.04100	0.02892	0.16205	0.00312	0.82032	0.02726	0.38309	0.01029	0.32321	0.00962
	Average		1.63E-08	6.50E-10	0.00457	0.00005	0.00400	0.00003	0.08182	0.00011	1.03779	0.00316	0.16172	0.00037	0.81718	0.00255	0.38220	0.00113	0.32205	0.00106
Paris 5	2.98	2.9	1.68E-08	5.44E-10	0.00457	0.00041	0.00399	0.00042	0.08197	0.00304	1.03843	0.03004	0.16139	0.00339	0.81516	0.02971	0.38226	0.01079	0.32160	0.00994
			1.68E-08	4.77E-10	0.00458	0.00038	0.00401	0.00039	0.08182	0.00276	1.03579	0.02142	0.16158	0.00229	0.81322	0.02003	0.38067	0.00885	0.32249	0.00702
			1.77E-08	6.32E-10	0.00452	0.00043	0.00393	0.00044	0.08193	0.00366	1.03559	0.03834	0.16219	0.00420	0.81877	0.03663	0.38174	0.01594	0.32023	0.01177
	Average		1.71E-08	7.02E-10	0.00455	0.00005	0.00398	0.00006	0.08191	0.00011	1.03660	0.00224	0.16172	0.00059	0.81571	0.00399	0.38156	0.00115	0.32144	0.00161

PT = petrologic type. Xenon abundances and isotopic compositions are computed from the average of 3–6 aliquots of gas taken from each sample. Errors are $2/\sqrt{(n-1)}$, where n is the number of duplicates.

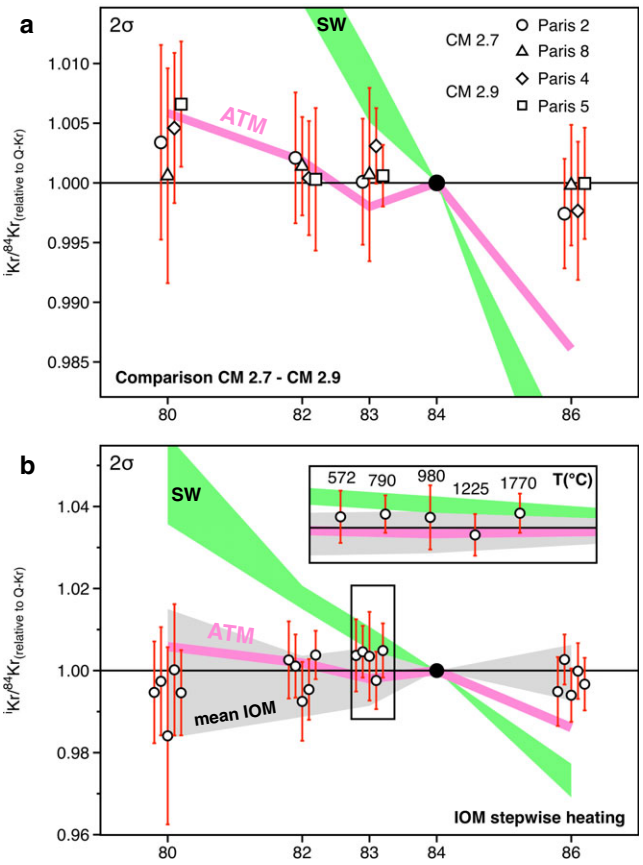

Fig. 3. Krypton isotopic spectra of the two CM 2.7 and CM 2.9 fragments (a) and of the IOM isolated from the Paris meteorite and analyzed by stepwise heating (b), normalized to the Q-phase composition (Busemann et al. 2000). Solar (Marti and Mathew 2015) and atmospheric (Basford et al. 1973) compositions are given for comparison. The gray area (b) corresponds to the abundance-weighted mean isotopic compositions of the Paris meteorite IOM. Corresponding data are given in Tables 4 and 5. Uncertainties are 2σ. (Color figure can be viewed at wileyonlinelibrary.com.)

~4.5 Ga, we calculated the amount of ^{136}Xe (mol) that has been produced by the spontaneous fission of ^{238}U for each fragment of the Paris meteorite analyzed in this study. Likewise, we use the initial ^{244}Pu/^{238}U of the meteorite and the branching ratio (fission/α-emission) of ^{244}Pu (0.125%, Fields et al. 1966) to calculate the initial contents of ^{244}Pu and determine the corresponding amounts of ^{136}Xe (mol) produced by spontaneous fission of now extinct ^{244}Pu. This calculation is strongly reliant on the value of the initial ^{244}Pu/^{238}U of the parent body. A low initial ^{244}Pu/^{238}U requires significant decay of ^{244}Pu before formation of the parent body. Increasing this time interval for decay might induce the initial amount of ^{129}I to be lower than the actual value (Hudson et al. 1989). Conversely, a high initial ^{244}Pu/^{238}U might require late inputs of freshly synthesized material in the early solar system. Here, if the widely adopted chondritic ^{244}Pu/^{238}U of 0.0068 ± 0.0010 (Hudson et al. 1989) is taken (in agreement with the recently determined value of 0.0061 ± 0.0028 for angrites; Nakashima et al. 2018), we observe that the Xe isotope corrections for contributions from ^{238}U and ^{244}Pu spontaneous fission are negligible (white symbols versus gray ones, Fig. S4 in supporting information). Two explanations can then be suggested: either there is an over-addition of some HL-Xe, or the initial ^{244}Pu/^{238}U ratio is underestimated. Interestingly, estimates of the initial ^{244}Pu/^{238}U of carbonaceous chondrites have been provided for Murchison (0.120 ± 0.011), Murray (0.132 ± 0.012), and Allende (0.113 ± 0.006) (mean value of 0.122; Kuroda and Myers 1991a, 1991b). These ^{244}Pu/^{238}U ratios are two orders of magnitude higher than the chondritic ratio given by Hudson et al. (1989). Nonetheless, Xe isotope spectra of the Paris meteorite corrected for contributions from ^{238}U and ^{244}Pu spontaneous fission (using a mean value of 0.122 for the initial ^{244}Pu/^{238}U) still exhibits ^{136}Xe excess relative to phase Q (black triangles, Fig. S4). Therefore, potential ^{244}Pu-derrived Xe cannot be distinguished on top of Q-Xe. The fact that a mix of 1.8% Xe-HL and 98.2% Q-Xe matches the bulk Xe isotope composition of the Paris meteorite suggests that excesses in the heavy isotopes ($^{132–136}$Xe) relative to Q-Xe as observed in CM 2.7 and CM 2.9 fragments would mainly be caused by the addition of Xe-H from nanodiamonds uniformly mixed with the rest of the solar system materials.

The composition of Q-Kr is consistent with a component produced in the early solar system by a series of mechanisms similar to those proposed to account for Xe-Q, i.e., mass-dependent fractionation of SW-Kr and addition of presolar components dominated by Kr-HL (Gilmour 2010). The fact that Kr isotope compositions measured here for the Paris meteorite are within error of Q-Kr with no deviation potentially carried by additional presolar contributions—as reported for Xe—may be attributed to a dilution effect linked to the fact that production of Q-Kr from fractionated SW-Kr requires a greater relative contribution from Kr-HL (~4.5%) than required from Xe-HL to produce Xe-Q from fractionated SW-Xe (~1.5%) (Gilmour 2010). Contrary to the case of Xe, presolar Kr associated with nanodiamonds may not be abundant enough, relative to Q-Kr, to be detectable. Interestingly, the high contribution of Xe-HL required to reproduce the Paris meteorite IOM data, relative to previously measured IOMs from carbonaceous and ordinary chondrites (Busemann et al. 2000), may be interpreted as evidence for a high contribution of presolar material (Fig. 7). The xenon isotopes of enstatite chondrites (Patzer and Schultz 2002), ureilites (Göbel et al. 1978) and carbonaceous chondrites (average carbonaceous chondrite composition, AVCC; Pepin 2003) appear to define a trend along a mixing line between mass fractionated solar wind (Gilmour 2010) and the pure Xe-

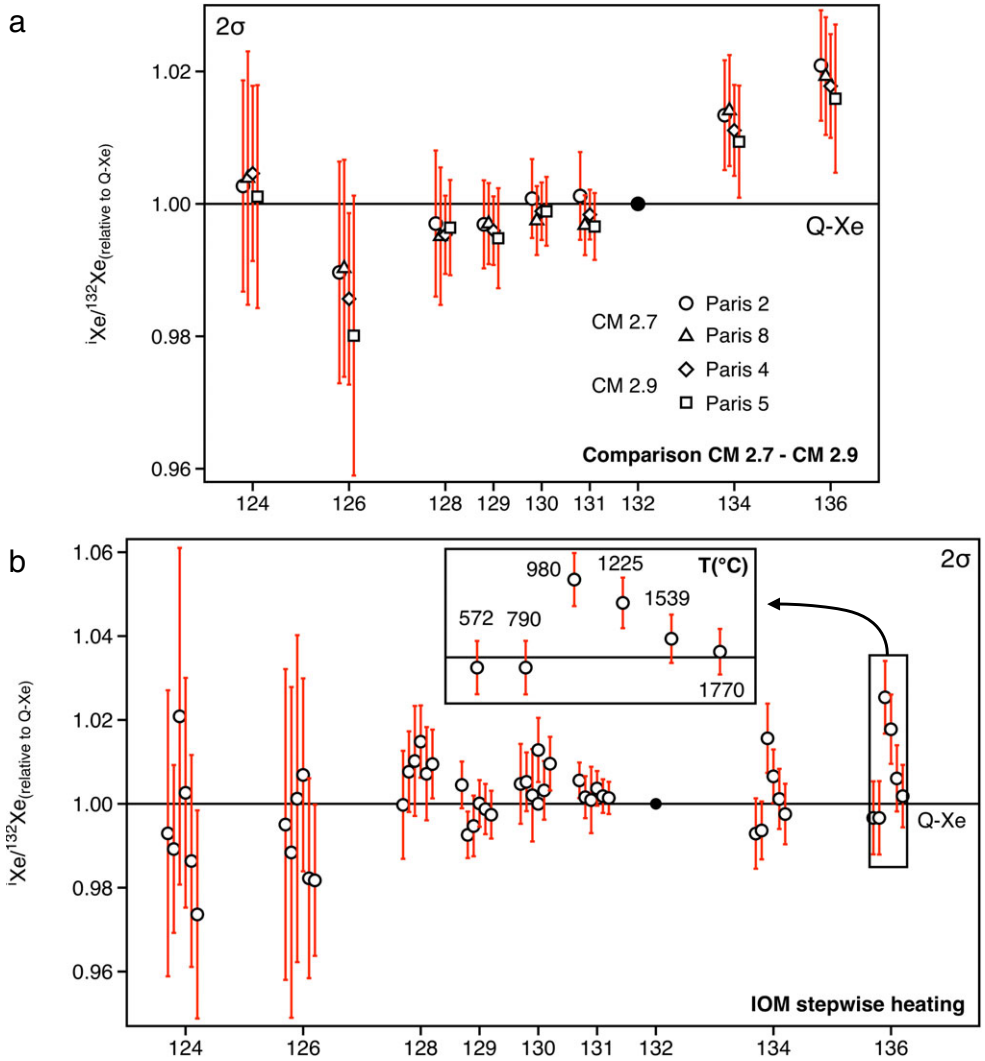

Fig. 4. Xenon isotopic spectra of the two CM 2.7 and CM 2.9 fragments (a) and of the IOM isolated from the Paris meteorite and analyzed by stepwise heating (b), normalized to the Q-phase composition (Busemann et al. 2000). For stepwise heating, isotopic ratios from increasing temperatures steps are displayed from left to right, as highlighted in the frame. The gray area (B) corresponds to the abundance-weighted mean isotopic compositions of the Paris meteorite IOM. Corresponding data are given in Tables 6 and 7. Uncertainties are 2σ. (Color figure can be viewed at wileyonlinelibrary.com.)

HL endmember (Huss and Lewis 1994). While Gilmour (2010) suggested that mixing of mass fractionated solar wind with Xe-HL might occur during processing on parent bodies, we propose that these might reveal a trend for increasing amounts of presolar materials with increasing heliocentric distance. Here, the bulk fragments of the Paris meteorite appear to contain an excess of 1.8% Xe-H, relative to Xe-Q, with negligible contribution from Xe-L (Fig. 4a). The occurrence of a heterogeneous distribution of presolar carriers enriched in nuclides produced in rapid neutron capture stars (r-process) has also been observed for molybdenum isotopes in carbonaceous chondrites relative to chondritic groups formed in the inner solar system (Dauphas et al. 2002; Kruijer et al. 2017). The r-process excess in carbonaceous chondrites suggests that there was an addition of a nucelosynthetically different component to the outer solar system prior to carbonaceous chondrite formation (Kruijer et al. 2017). It is important to distinguish between the fraction of presolar material in bulk samples and the proportion of Xe-HL added to fractionated solar wind to produce the IOM signatures (Fig. 7). Bulk Xe compositions (e.g., AVCC, enstatite chondrites, ureilites, and bulk fragments of the Paris meteorite; Fig. 7) depend on the abundance of presolar material and concentration of Xe therein, the IOM abundance, and concentration/composition of Xe in "phase Q," as well as on any Xe component in other phases. This can therefore be affected by the extent of

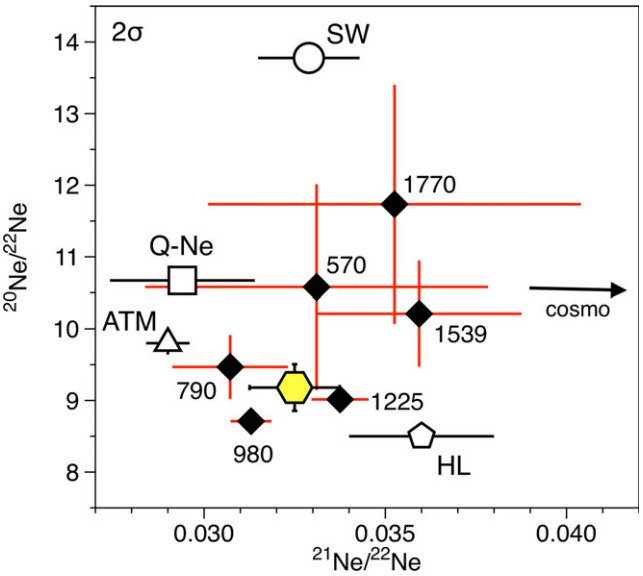

Fig. 5. Neon three-isotope diagram of the Paris meteorite's IOM upon stepwise heating. The temperature associated to each step is given next to the corresponding data point. The abundance-weighted mean isotopic composition of the Paris meteorite IOM corresponds to the yellow hexagon. Corresponding data are given in Table 1. SW = solar wind (Heber et al. 2012); ATM = terrestrial atmosphere (Ozima and Podosek 2002); Q-Ne: (Busemann et al. 2000), HL-Ne: (Huss and Lewis 1994), cosmo: typical chondritic value for the cosmogenic galactic cosmic ray endmember (Busemann et al. 2000). Uncertainties are 2σ. (Color figure can be viewed at wileyonlinelibrary.com.)

thermal processing and/or physical separation of HL-bearing phases. On the other hand, the end product of Q process(es) trapping ionized Xe into organic matter with mass fractionation would depend on the composition of the ambient gas it was trapped from, and perhaps subsequent parent body incorporation of HL or mixing with some HL-bearing phases.

Origin of Chondritic Noble Gases and Their Evolution During Alteration

The exact host phase(s) of Q-gases in chondrites, although not precisely defined (Marrocchi et al. 2015), appears to be closely related to refractory organic compounds (Ott et al. 1981; Busemann et al. 2000). A presolar origin of phase Q inherited from the molecular cloud from which the Sun was later formed has been proposed to explain its association with presolar materials (Huss and Alexander 1987). An alternative view considers Q as being locally derived from an initial nebula mix now represented by the solar composition. It has been demonstrated that ~2% of Xe-H apparently present in phase Q may not be necessarily originated from stellar nucleosythesis (Meshik et al. 2016), but could result from the addition of xenon originating from chemically fractionated fission (CFF) of ^{244}Pu, which was extant during the formation of phase Q. This nucleo-chemical process typically yields ^{136}Xe to ^{134}Xe in 2:1 proportion, with little ^{132}Xe and ^{131}Xe, and no lighter isotopes, which are shielded from fission by stable isobars. This interpretation implies that phase Q is of solar, rather than of presolar origin (Meshik et al. 2016). Processes involved in the origin of Q-Xe have been investigated by plasma experiments dedicated to study the adsorption of Xe onto organics defects (Marrocchi et al. 2011) and the incorporation of fractionated noble gases during organosynthesis (Kuga et al. 2015). These two studies support a scenario in which organic materials would constitute the main carrier phase of chondritic noble gases in meteorites, with a likely common and pre-asteroidal origin (Kuga et al. 2015).

No difference was found between the Kr and Xe isotopes of the CM 2.9 and CM 2.7 fragments. This result is consistent with the lack of significant difference in the in situ molecular signature (X-ray absorption near edge structure spectra) of the organic matter contained in the least (CM 2.9) and most altered (CM 2.7) regions of the Paris meteorite matrix (Vinogradoff et al. 2017). According to Vinogradoff et al. (2017), the Paris (~2.8 CM) and Murchison (CM 2.5) IOM exhibit distinct molecular and structural signatures, as a result of hydrothermal alteration. Taken together, these results indicate that the main carrier phases of heavy noble gases were not significantly affected by the episode of hydrothermal alteration on the parent body of the Paris meteorite.

A dual origin has been proposed for the ice grains accreted by the Paris meteorite parent body, with evidence for O and H isotope signatures from both local (i.e., inner solar system) and outer solar system water ices (Vacher et al. 2016; Piani et al. 2018). Yet, we found that such a contribution of outer solar system water ice (taken with a composition similar to that of comet 67P/G; Marty et al. 2017) could only contribute <1% of the total budget of ^{132}Xe in the Paris meteorite. Shifts of the Xe heavy isotope ratios toward lower values, as expected in the case of a contribution from cometary-like Xe (Fig. 2), may be overprinted by heavy Xe isotope excesses of nucleosynthetic origin. Another possibility is that cometary-like Xe associated with the outer solar system water ice component may have been lost to space during ice melting. In this case, Xe retained in refractory organic materials would have been preserved only, without having exchanged with Xe carried by alteration fluids.

The ubiquity of the Q-phase associated with IOM implies that either (1) the IOM in carbonaceous chondrites is inherited from a unique process of organosynthesis resulting in noble gases being trapped in IOM with a Q-like signature, or (2) that several distinct

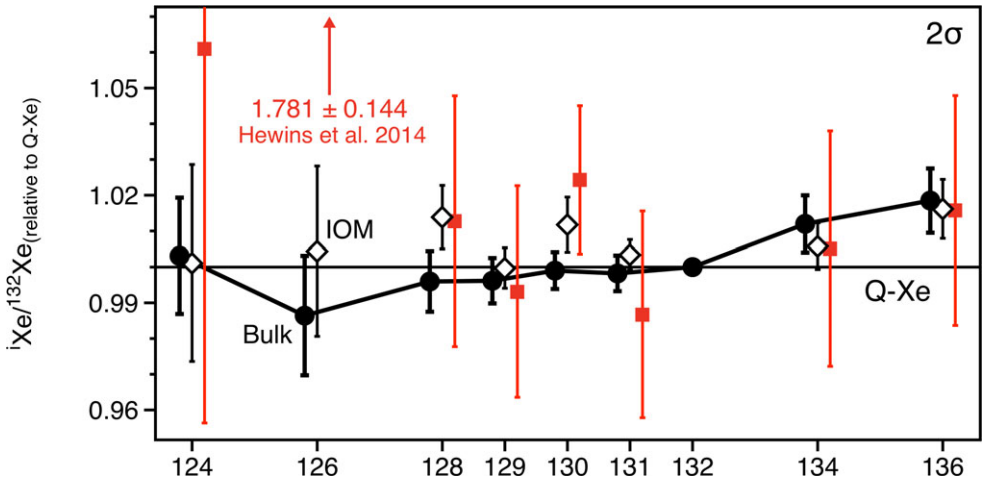

Fig. 6. Xenon isotopic spectra of the CM 2.7 and CM 2.9 fragments normalized to the Q-phase composition from Busemann et al. (2000) and compared to the bulk Xe isotope composition determined by Hewins et al. (2014). Atmospheric Xe is also given for comparison (Basford et al. 1973). Uncertainties are 2σ. (Color figure can be viewed at wileyonlinelibrary.com.)

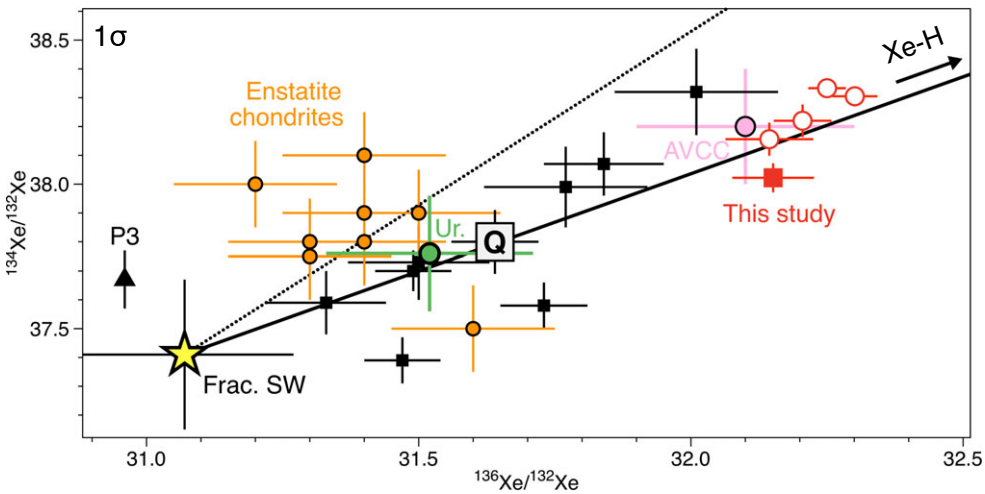

Fig. 7. Xenon three-isotope diagram ($^{134}Xe/^{132}Xe$ versus $^{136}Xe/^{132}Xe$) of the Paris meteorite's IOM and bulk fragments. The composition of Xe-Q (gray square, Busemann et al. 2000) is the average and standard error of compositions measured in IOMs from nine meteorites (black squares, Busemann et al. 2000). This accepted Xe-Q composition is accounted for by mixing of mass fractionated solar wind (Frac. SW) with Xe-HL (here Xe-H, see fig. 4 from Gilmour 2010). Bulk compositions of enstatite chondrites (circles filled with orange, Patzer and Schultz 2002), ureilites (circle filled with green, Göbel et al. 1978), carbonaceous chondrites (circle filled with pink, average carbonaceous chondrite composition, AVCC; Pepin 2003), and Paris meteorite bulk fragments (red open circles) appear to fall along this trend. The abundance-weighted mean isotopic composition of the Paris meteorite IOM (red square) also falls along this trend, with evidence for a high fraction of Xe-H relative to other IOMs from carbonaceous and ordinary chondrites (black squares, Busemann et al. 2000). P3: presolar component released at relatively low temperature in nanodiamonds (Gilmour 2010). Uncertainties are 1σ. (Color figure can be viewed at wileyonlinelibrary.com.)

mechanisms of IOM synthesis (e.g., in the protosolar nebula (Remusat et al. 2006, 2009; Kuga et al. 2015), in the interstellar medium (Robert and Epstein 1982; De Marcellus et al. 2016) or on asteroids (Kebukawa et al. 2017; Vinogradoff et al. 2018) are able to yield a Q-like signature for noble gases. Interestingly, the trapping efficiency of Xe neutrals in organics is very low and does not induce measurable isotopic fractionation without ionization (Marrocchi and Marty 2013). Under ionizing conditions, the trapping efficiency of Xe ions reproduces the Xe isotope fractionation and the high xenon concentration measured in phase Q of primitive meteorites (Marrocchi et al. 2011; Kuga et al. 2015). To date and to our knowledge, organosynthesis in the ionized gas phase of the protosolar nebula (Kuga et al. 2015) is the only mechanism that accounts for the formation of an IOM carrying noble gases with Q-like elemental and isotopic fractionation patterns.

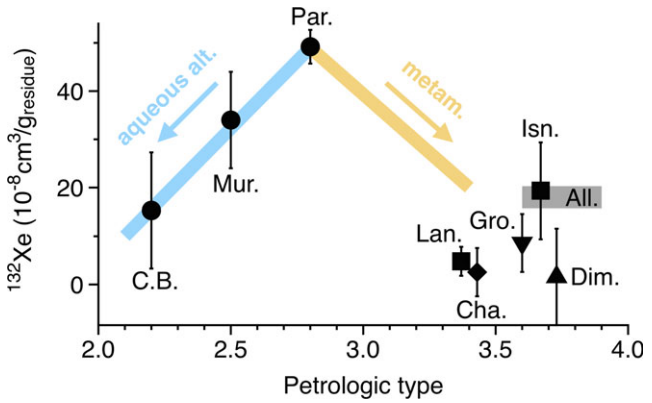

Fig. 8. ^{132}Xe contents (10^{-8} cm^3 g^{-1} $_{residue}$) of different IOM isolated from carbonaceous chondrite (Busemann et al. 2000) (from left to right, CM 2.2: Cold Bokkeveld; CM 2.5: Murchison; CM 2.8: Paris [this study]; CO 3.4: Lancé; LL 3.4: Chainpur; CV 3.6: Grosnaja; CV >3.6: Allende [petrologic type from; Bonal et al. 2006]; CO 3.7: Isna; H 3.7: Dimmit). Pathways of Xe loss upon aqueous alteration (aqueous alt.) and metamorphism (metam.), as hypothesized by Busemann et al. (2000), are displayed. Symbols refer to petrologic types (circles: CM, squares: CO, triangle pointing downward: CV, triangle pointing upward: H, diamond: LL). Uncertainties are 1σ. (Color figure can be viewed at wileyonlinelibrary.com.)

Recently, Fray et al. (2016) reported the in situ detection of solid organic matter similar to the insoluble organic matter found in the carbonaceous chondrite meteorites in the dust particles emitted by comet 67P/Churyumov–Gerasimenko. We speculate that, if the IOM present in carbonaceous chondrites were contributed by at least two isotopically distinct reservoirs (e.g., a Q-like inner solar system component and an outer solar system reservoir), then a mixing between the two signatures should be observed in meteorites with different proportions of these two endmembers. This is, however, not observed in the Paris meteorite. The noble gas signature of Paris can therefore be defined as dominantly Q-like. The ubiquity of Q-like noble gases in the IOM of carbonaceous chondrites suggests that either (1) noble gases associated with cometary IOM are also Q-like (with a common origin—solar or interstellar—for the IOM in meteorites and comets) such that an addition of cometary material cannot be resolved using the noble gases or (2) cometary IOM is poor in noble gases, so that mixing with Q-like inner solar system IOM results in an unchanged Q noble gas signature. A comet sample-return mission allowing the IOM of cometary samples to be isolated and measured in the laboratory for its heavy noble gas isotopes would potentially be able to resolve these issues. Likewise, the possibility of forming a Q-like elementary and isotopic noble gas composition trapped in organic materials synthesized from the photochemical and thermal processing of interstellar ice analogues appears to be a promising avenue of investigation.

Our data indicate that Xe isotopes probably remained unaffected by the limited episode of aqueous alteration that occurred on the parent body of the Paris meteorite. To this extent, the ^{132}Xe concentrations we report for the IOM of the Paris meteorite are the highest yet measured for the IOM of carbonaceous chondrites (Fig. 8). From a simple mass balance, we find that the Paris meteorite's IOM, which constitutes <2 wt% of the bulk sample (see the Preparation of the Insoluble Organic Residue section), contains more than 50% of the total amount of Xe present in the meteorite. The mass of the residue depends on the cleanliness, abundance of gas-lacking phases, and perhaps the procedure to produce the residue. The noble gas bearing Q (and diamonds) may also contribute only <1% to the total mass of the residue. However, by considering that (1) all IOM in carbonaceous chondrites inherited a similar phase Q component, and that (2) variations of the ^{132}Xe content in carbonaceous chondrites are a function of the degree of secondary processing (thermal metamorphism and aqueous alteration; Busemann et al. 2000), we conclude that the Paris meteorite likely carries the most pristine chondritic IOM observed to date. This is in line with infrared and Raman microspectroscopy observations of the Paris meteorite organic signature, which show that the Paris meteorite has suffered minimal thermal metamorphism as well as weak aqueous alteration, leaving even the possibility to have preserved some organic matter of interstellar origin (Merouane et al. 2012). The chemistry of the Paris meteorite may thus be closely related to the early stages of the solar nebula. This is further supported by the low contents of amino acids and lack of alkylated PAHs in the Paris meteorite, the abundance and distribution of both types of molecules likely being related to episodes of aqueous alteration within carbonaceous asteroids (Martins et al. 2015). This is also in agreement with the solid-state ^{13}C nuclear magnetic resonance and electron paramagnetic resonance spectra of the Paris IOM, which show a higher proportion of aliphatic carbons and organic radicals relative to the Murchison IOM (Vinogradoff et al. 2017).

Nonetheless, we find that the ^{36}Ar/^{132}Xe ratios—which reflect the degree of secondary processing (Busemann et al. 2000)—are slightly lower in the CM 2.7 fragments relative to the CM 2.9 ones (Table 8), probably related to a preferential loss of the lightest noble gases upon aqueous alteration. Alternatively, several studies suggested that phase Q may consist of an assemblage of carrier phases and substructures that would exhibit variable resistance to alteration processes, and contain variable proportions of light and heavy noble gases (Gros and Anders 1977; Busemann et al. 2000; Marrocchi et al. 2005, 2015). A preferential loss

Table 8. Elemental composition of the Paris meteorite IOM and bulk fragments. Elemental composition of Q (Busemann et al. 2000) and bulk fragments of the Paris meteorite from Hewins et al. (2014) are given for comparison. The factor ~6 between bulk $^{36}Ar/^{132}Xe$ measured in this study and analyzed by Hewins et al. (2014) might illustrate a certain degree of inhomogeneity for noble gases concentrations in Paris at the mg scale.

		$^{20}Ne/^{36}Ar$	±2σ	$^{20}Ne/^{132}Xe$	±2σ	$^{36}Ar/^{132}Xe$	±2σ	$^{84}Kr/^{132}Xe$	±2σ
IOM	572	0.455	0.099	8.587	1.880	18.881	4.158	1.097	0.242
	790	0.171	0.029	19.307	3.801	112.871	22.089	1.149	0.254
	980	0.488	0.089	57.111	10.684	117.037	21.745	0.718	0.135
	1225	0.168	0.031	1.150	0.213	6.854	1.284	0.709	0.133
	1539	0.416	0.078	7.758	1.517	18.667	3.652	–	–
	1770	0.103	0.020	3.500	0.703	34.105	6.803	0.879	0.176
	Total	0.254	0.047	3.476	0.649	13.679	2.556	0.707	0.134
			Bulk	CM2.7	Paris 2	78.723	6.227	0.734	0.056
					Paris 8	92.593	5.891	0.784	0.038
				CM2.9	Paris 4	114.724	8.255	0.847	0.058
					Paris 5	108.187	7.865	0.836	0.056
Hewins et al. 2014 (a)		1.42	0.02	–	–	–	–	–	–
Hewins et al. 2014 (b)		0.82	0.02	408.332	46.309	583.684	13.92	–	–
Q		0.044	0.012	3.2	1	76	14	0.81	0.1

of Ar relative to Xe during aqueous alteration could thus be related to the destruction of poorly resistant phases with high Ar/Xe during early aqueous alteration. Regardless of the alteration or metamorphism degree, the isotopic ratios of phase Q from different meteorites are similar and should therefore be identical to the originally incorporated Q composition (Busemann et al. 2000).

CONCLUSION

Because the Paris meteorite parent body locally accreted only limited amounts of water ice, part of the materials constituting this meteorite have been exceptionally well preserved from secondary processing by aqueous alteration. Recently, O and H isotopic evidence for a contribution of outer solar system water ice have been found in this meteorite (Vacher et al. 2016; Piani et al. 2018). We separately analyzed pristine CM 2.9 fragments, CM 2.7 fragments, and the IOM of the Paris meteorite for their heavy noble gas isotope compositions but found no evidence for a contribution of an outer solar system noble gas component (supposed to be cometary-like; Marty et al. 2017). All our noble gas isotope data point to phase Q being the dominating carrier of noble gases, with small excesses in the heavy Xe isotopes relative to phase Q in the bulk samples being attributed to a contribution of presolar materials (r-process isotopes; Gilmour and Turner 2007). The ubiquity of the Q-phase in meteorites suggests that noble gases possibly present in cometary insoluble organic matter (Fray et al. 2016) could potentially also have Q-like signatures and be of nebular origin. The fact that no difference in the elementary and isotopic composition of Xe could be found between CM 2.9 and CM 2.7 fragments agree with the observation that the IOM (the main carrier of heavy noble gases in chondrites) shows little variation in X-ray absorption near edge structure spectroscopy between fresh and altered areas (Vinogradoff et al. 2017). The high concentration \of Xe in the Paris meteorite IOM relative to other carbonaceous chondrites' IOM also correlates with the Paris meteorite carrying the most pristine IOM and exhibiting the lowest degree of secondary processing (thermal metamorphism and aqueous alteration; Busemann et al. 2000) observed so far in meteorites (Hewins et al. 2014).

Acknowledgments—We are grateful to Brigitte Zanda who initiated a stimulating research project on the Paris meteorite, and to the Museum National d'Histoire Naturelle de Paris for allocation of this precious sample. Laurette Piani and Michael Broadley are thanked for fruitful discussions. We thank the two reviewers, Jamie Gilmour and Henner Busemann, for their constructive and insightful comments. This study was supported by the European Research Council (grant no. 695618). This is a CRPG contribution #2595.

Editorial Handling—Dr. Ingo Leya

REFERENCES

Alexander C. M. O'D., Bowden R., Fogel M. L., Howard K. T., Herd C. D. K., and Nittler L. R. 2012. The provenances of asteroids, and their contributions to the volatile inventories of the terrestrial planets. *Science* 337:721–723.

Basford J. R., Dragon J. C., Pepin R. O., Coscio M. R. Jr., and Murthy V. R. 1973. Krypton and xenon in lunar fines. Proceedings, 4th Lunar Science Conference. pp. 1915–1955.

Bekaert D. V., Avice G., Marty B., Henderson B., and Gudipati M. S. 2017. Stepwise heating of lunar anorthosites 60025, 60215, 65315 possibly reveals an indigenous noble gas component on the Moon. *Geochimica et Cosmochimica Acta* 218:114–131.

Bitsch B., Johansen A., Lambrechts M., and Morbidelli A. 2015. The structure of protoplanetary discs around evolving young stars. *Astronomy & Astrophysics* 575:A28. https://doi.org/10.1051/0004-6361/201424964.

Bland P. A., Jackson M. D., Coker R. F., Cohen B. A., Webber J. B. W., Lee M. R., Duffy C. M., Chater R. J., Ardakani M. G., McPhail D. S., and McComb D. W. 2009. Why aqueous alteration in asteroids was isochemical: High porosity ≠ high permeability. *Earth and Planetary Science Letters* 287:559–568.

Bonal L., Quirico E., Bourot-Denise M., and Montagnac G. 2006. Determination of the petrologic type of CV3 chondrites by Raman spectroscopy of included organic matter. *Geochimica et Cosmochimica Acta* 70:1849–1863.

Brearley A. J. 2006. The action of water. In *Meteorites and the early solar system II*, edited by Dante L. and McSween H.Y. Jr. Tucson, Arizona: University of Arizona Press. pp. 587–624.

Browning L. B., McSween H. Y., and Zolensky M. E. 1996. Correlated alteration effects in CM carbonaceous chondrites. *Geochimica et Cosmochimica Acta* 60:2621–2633.

Busemann H., Baur H., and Wieler R. 2000. Primordial noble gases in "phase Q" in carbonaceous and ordinary chondrites studied by closed-system stepped etching. *Meteoritics & Planetary Science* 35:949–973.

Cleeves L. I., Bergin E. A., Alexander C. M. O'D., Du F., Graninger D., Öberg K. I., and Harries T. J. 2014. The ancient heritage of water ice in the solar system. *Science* 345:1590–1593.

Crowther S. A. and Gilmour J. D. 2013. The Genesis solar xenon composition and its relationship to planetary xenon signatures. *Geochimica et Cosmochimica Acta* 123:17–34.

Dauphas N., Marty B., and Reisberg L. 2002. Molybdenum evidence for inherited planetary scale isotope heterogeneity of the protosolar nebula. *The Astrophysical Journal* 565:640.

De Marcellus P., Fresneau A., Brunetto R., Danger G., Duvernay F., Meinert C., Meierhenrich U. J., Borondics F., Chiavassa T., and Le Sergeant d' Hendecourt L. 2016. Photo and thermochemical evolution of astrophysical ice analogues as a source for soluble and insoluble organic materials in solar system minor bodies. *Monthly Notices of the Royal Astronomical Society* 464:114–120.

Drake M. J. 2005. Origin of water in the terrestrial planets. *Meteoritics & Planetary Science* 40:519–527.

Fields P. R., Friedman A. M., Milsted J., Lerner J., Stevens C. M., Metta D., and Sabine W. K. 1966. Decay properties of plutonium-244, and comments on its existence in nature. *Nature* 212:131.

Fray N., Bardyn A., Cottin H., Altwegg K., Baklouti D., Briois C., Colangeli L., Engrand C., Fischer H., Glasmachers A., Grün E., Haerendel G., Henkel H., Höfner H., Hornung K., Jessberger E. K., Koch A., Krüger H., Langevin Y., Lehto H., Lehto K., Le Roy L., Merouane S., Modica P., Orthous-Daunay F.-R., Paquette J., Raulin F., Rynö J., Schulz R., Silén J., Siljeström S., Steiger W., Stenzel O., Stephan T., Thirkell L., Thomas R., Torkar K., Varmuza K., Wanczek K.-P., Zaprudin B., Kissel J., and Hilchenbach M. 2016. High-molecular-weight organic matter in the particles of comet 67P/Churyumov–Gerasimenko. *Nature* 538:72–74.

Gilmour J. D. 2010. "Planetary" noble gas components and the nucleosynthesis history of solar system material. *Geochimica et Cosmochimica Acta* 74:380–393.

Gilmour J. D. and Turner G. 2007. Constraints on nucleosynthesis from xenon isotopes in presolar material. *The Astrophysical Journal* 657:600.

Gilmour J. D., Verchovsky A. B., Fisenko A. V., Holland G., and Turner G. 2005. Xenon isotopes in size separated nanodiamonds from Efremovka: 129Xe*, Xe-P3, and Xe-P6. *Geochimica et cosmochimica acta* 69:4133–4148.

Göbel R., Ott U., and Begemann F. 1978. On trapped noble gases in ureilites. *Journal of Geophysical Research: Solid Earth* 83:855–867.

Gros J. and Anders E. 1977. Gas-rich minerals in the Allende meteorite: Attempted chemical characterization. *Earth and Planetary Science Letters* 33:401–406.

Heber V. S., Baur H., Bochsler P., McKeegan K. D., Neugebauer M., Reisenfeld D. B., Wieler R., and Wiens R. C. 2012. Isotopic mass fractionation of solar wind: Evidencefrom fast and slow solar wind collected by the Genesis mission. *The Astrophysical Journal* 759:121.

Hewins R. H., Bourot-Denise M., Zanda B., Leroux H., Barrat J.-A., Humayun M., Göpel C., Greenwood R. C., Franchi I. A., Pont S., Lorand J.-P., Cournède C., Gattacceca J., Rochette P., Kuga M., Marrocchi Y., and Marty B. 2014. The Paris meteorite, the least altered CM chondrite so far. *Geochimica et Cosmochimica Acta* 124:190–222.

Hudson G. B., Kennedy B. M., Podosek F. A., and Hohenberg C. M. 1989. The early solar system abundance of Pu-244 as inferred from the St. Severin chondrite. Proceedings, 19th Lunar and Planetary Science Conference. pp. 547–557.

Humbert F., Libourel G., France-Lanord C., Zimmermann L., and Marty B. 2000. CO2-laser extraction-static mass spectrometry analysis of ultra- low concentrations of nitrogen in silicates. *Geostandards Newsletter* 24:255–260.

Huss G. R. and Alexander E. C. 1987. On the presolar origin of the "normal planetary" noble gas component in meteorites. *Journal of Geophysical Research: Solid Earth* 92:E710–E716.

Huss G. R. and Lewis R. S. 1994. Noble gases in presolar diamonds I: Three distinct components and their implications for diamond origins. *Meteoritics & Planetary Science* 29:791–810.

Huss G. R., Lewis R. S., and Hemkin S. 1996. The normal planetary noble gas component in primitive chondrites: Compositions, carrier, and metamorphic history. *Geochimica et Cosmochimica Acta* 60:3311–3340.

Kebukawa Y., Chan Q. H., Tachibana S., Kobayashi K., and Zolensky M. E. 2017. One-pot synthesis of amino acid precursors with insoluble organic matter in planetesimals with aqueous activity. *Science Advances* 3:e1602093.

Kruijer T. S., Burkhardt C., Budde G., and Kleine T. 2017. Age of Jupiter inferred from the distinct genetics and formation times of meteorites. *Proceedings of the National Academy of Sciences* 114:6712–6716.

Kuga M., Marty B., Marrocchi Y., and Tissandier L. 2015. Synthesis of refractory organic matter in the ionized gas phase of the solar nebula. *Proceedings of the National Academy of Sciences* 112:7129–7134.

Kuroda P. and Myers W. 1991a. Plutonium-244 dating I. Initial ratio of plutonium to uranium in the Allende meteorite. *Journal of Radioanalytical and Nuclear Chemistry* 150:35–51.

Kuroda P. and Myers W. 1991b. Plutonium-244 dating: II. Initial ratios of plutonium to uranium in the Murray and Murchison meteorites. *Journal of Radioanalytical and Nuclear Chemistry* 150:53–69.

Lavielle B. and Marti K. 1992. Trapped xenon in ordinary chondrites. *Journal of Geophysical Research* 97:20875–20881.

Le Guillou C. and Brearley A. 2014. Relationships between organics, water and early stages of aqueous alteration in the pristine CR3. 0 chondrite MET 00426. *Geochimica et Cosmochimica Acta* 131:344–367.

Lecar M., Podolak M., Sasselov D., and Chiang E. 2006. On the location of the snow line in a protoplanetary disk. *The Astrophysical Journal* 640:1115.

Lee J. Y., Marti K., Severinghaus J. P., Kawamura K., Yoo H. S., Lee J. B., and Kim J. S. 2006. A redetermination of the isotopic abundances of atmospheric Ar. *Geochimica et Cosmochimica Acta* 70:4507–4512.

Leroux H., Cuvillier P., Zanda B., and Hewins R. H. 2015. GEMS-like material in the matrix of the Paris meteorite and the early stages of alteration of CM chondrites. *Geochimica et Cosmochimica Acta* 170:247–265.

Lewis R. S., Ming T., Wacker J. F., Anders E., and Steel E. 1987. Interstellar diamonds in meteorites. *Nature* 326:160.

Lunine J. I. 2006. Origin of water ice in the solar system. In *Meteorites and the early solar system II*, edited by Lauretta D. S. and McSween H. Y. Tucson, Arizona: The University of Arizona Press. pp. 309–318.

Lyons J. R. and Young E. D. 2005. CO self-shielding as the origin of oxygen isotope anomalies in the early solar nebula. *Nature* 435:317–320.

Mabry J. C., Meshik A. P., Hohenberg C. M., Marrocchi Y., Pravdivtseva O. V., Wiens R. C., Olinger C., Reisenfeld D. B., Allton J., Bastien R., McNamara K., Stansbery E., and Burnett D. S. 2007. Refinement and implications of noble gas measurements from Genesis (abstract #1338). 38th Lunar and Planetary Science Conference. CD-ROM.

Marrocchi Y. and Marty B. 2013. Experimental determination of the xenon isotopic fractionation during adsorption. *Geophysical Research Letters* 40:4165–4170.

Marrocchi Y., Derenne S., Marty B., and Robert F. 2005. Interlayer trapping of noble gases in insoluble organic matter of primitive meteorites. *Earth and Planetary Science Letters* 236:569–578.

Marrocchi Y., Marty B., Reinhardt P., and Robert F. 2011. Adsorption of xenon ions onto defects in organic surfaces: Implications for the origin and the nature of organics in primitive meteorites. *Geochimica et Cosmochimica Acta* 75:6255–6266.

Marrocchi Y., Gounelle M., Blanchard I., Caste F., and Kearsley A. T. 2014. The Paris CM chondrite: Secondary minerals and asteroidal processing. *Meteoritics & Planetary Science* 49:1232–1249.

Marrocchi Y., Avice G., and Estrade N. 2015. Multiple carriers of Q noble gases in primitive meteorites. *Geophysical Research Letters* 42:2093–2099.

Marrocchi Y., Bekaert D. V., and Piani L. 2018. Origin and abundance of water in carbonaceous asteroids. *Earth and Planetary Science Letters* 482:23–32.

Marti K. and Mathew K. J. 1998. Noble gas components in planetary atmospheres and interiors in relation to solar wind and meteorites. *Earth and Planetary Sciences* 107:425–431.

Marti K. and Mathew K. J. 2015. Xenon in the protoplanetary disk (PPD-XE). *The Astrophysical Journal Letters* 806:L30.

Martins Z., Modica P., Zanda B., and d'Hendecourt L. L. S. 2015. The amino acid and hydrocarbon contents of the Paris meteorite: Insights into the most primitive CM chondrite. *Meteoritics & Planetary Science* 50:926–943.

Marty B., Altwegg K., Balsiger H., Bar-Nun A., Bekaert D. V., Berthelier J.-J., Bieler A., Briois C., Calmonte U., Combi M., De Keyser J., Fiethe B., Fuselier S. A., Gasc S., Gombosi T. I., Hansen K. C., Hässig M., Jäckel A., Kopp E., Korth A., Le Roy L., Mall U., Mousis O., Owen T., Rème H., Rubin M., Sémon T., Tzou C.-Y., Waite J. H., and Wurz P. 2017. Xenon isotopes in 67P/Churyumov-Gerasimenko show that comets contributed to Earth's atmosphere. *Science* 356:1069–1072.

Merouane S., Djouadi Z., d'Hendecourt L. L. S., Zanda B., and Borg J. 2012. Hydrocarbon materials of likely interstellar origin from the Paris meteorite. *The Astrophysical Journal* 756:154.

Meshik A. P., Pravdivtseva O. V., and Hohenberg C. M. 2001. Selective laser extraction of Xe-H from Xe-HL in meteoritic nanodiamonds: real effect or experimental artefact? (abstract #2158). 32nd Lunar and Planetary Science Conference. CD-ROM.

Meshik A., Mabry J., Hohenberg C., Marrocchi Y., Pravditseva O., Burnett D. S., Olinger C., Wiens R. C., Reisenfeld D., Allton J., McNamara K., Stansbery E., and Jurewicz A. J. G. 2007. Constraints on Ne and Ar fractionation in the solar wind. *Science* 318:433–435.

Meshik A., Hohenberg C., Pravdivtseva O., and Burnett D. 2014. Heavy noble gases in solar wind delivered by Genesis Mission. *Geochimica et Cosmochimica Acta* 45:1751–1788.

Meshik A. P., Pravdivtseva O. V., and Hohenberg C. M. 2016. New evidence for chemical fractionation of radioactive xenon precursors in fission chains. *Physical Review C* 93: 044614.

Nakashima D., Nagao K., and Irving A. J. 2018. Noble gases in angrites Northwest Africa 1296, 2999/4931, 4590, and 4801: Evolution history inferred from noble gas signatures. *Meteoritics & Planetary Science* 53:952–972.

Ott U. 1996. Interstellar diamond xenon and timescales of supernova ejecta. *The Astrophysical Journal* 463:344.

Ott U. 2014. Planetary and pre-solar noble gases in meteorites. *Chemie der Erde-Geochemistry* 74:519–544.

Ott U., Mack R., and Sherwood C. 1981. Noble-gas-rich separates from the Allende meteorite. *Geochimica et Cosmochimica Acta* 45:1751–1788.

Ozima M. and Podosek F. A. 2002. *Noble gas geochemistry*. Cambridge: Cambridge University Press.

Palguta J., Schubert G., and Travis B. J. 2010. Fluid flow and chemical alteration in carbonaceous chondrite parent bodies. *Earth and Planetary Science Letters* 296:235–243.

Patzer A. and Schultz L. 2002. Noble gases in enstatite chondrites II: The trapped component. *Meteoritics & Planetary Science* 37:601–612.

Pepin R. O. 2003. On noble gas processing in the solar accretion disk. *Space Science Reviews* 106:211–230.

Piani L., Robert F., and Remusat L. 2015. Micron-scale D/H heterogeneity in chondrite matrices: A signature of the pristine solar system water? *Earth and Planetary Science Letters* 415:154–164.

Piani L., Yurimoto H., and Remusat L. 2018. A dual origin for water in carbonaceous asteroids revealed by CM chondrites. *Nature Astronomy* 2:317–323.

Pignatelli I., Marrocchi Y., Vacher L., Delon R., and Gounelle M. 2016. Multiple precursors of secondary mineralogical assemblages in CM chondrites. *Meteoritics & Planetary Science* 51:785–805.

Pignatelli I., Marrocchi Y., Mugnaioli E., Bourdelle F., and Gounelle M. 2017. Mineralogical, crystallographic and redox features of the earliest stages of fluid alteration in CM chondrites. *Geochimica et Cosmochimica Acta* 209:106–122.

Porcelli D. and Ballentine C. J. 2002. An overview of noble gas geochemistry and cosmochemistry. *Reviews in Mineralogy and Geochemistry* 47:1–19.

Ragettli R. A., Hebeda E. H., Signer P., and Wieler R. 1994. Uranium-xenon chronology: Precise determination of $\lambda sf*$ 136Ys*f* for spontaneous fission of 238U. *Earth and Planetary Science Letters* 128:653–670.

Remusat L., Derenne S., Robert F., and Knicker H. 2005. New pyrolytic and spectroscopic data on Orgueil and murchison insoluble organic matter: A different origin than soluble? *Geochimica et Cosmochimica Acta* 69:3919–3932.

Remusat L., Palhol F., Robert F., Derenne S., and France-Lanord C. 2006. Enrichment of deuterium in insoluble organic matter from primitive meteorites: A solar system origin?. *Earth and Planetary Science Letters* 243:15–25.

Remusat L., Le Guillou C., Rouzaud J.-N., Binet L., Derenne S., and Robert F. 2008. Molecular study of insoluble organic matter in kainsaz CO3 carbonaceous chondrite: Comparison with CI and CM IOM. *Meteoritics & Planetary Science* 43:1099–1111.

Remusat L., Robert F., Meibom A., Mostefaoui S., Delpoux O., Binet L., Gourier D., and Derenne S. 2009. Protoplanetary disk chemistry recorded by D-rich organic radicals in carbonaceous chondrites. *The Astrophysical Journal* 698:2087.

Reynolds J. H. and Turner G. 1964. Rare gases in the chondrite Renazzo. *Journal of Geophysical Research* 69:3263–3281.

Riebe M. E., Busemann H., Wieler R., and Maden C. 2017. Closed system step etching of CI chondrite Ivuna reveals primordial noble gases in the HF-solubles. *Geochimica et Cosmochimica Acta* 205:65–83.

Robert F. and Epstein S. 1982. The concentration and isotopic composition of hydrogen, carbon and nitrogen in carbonaceous meteorites. *Geochimica et Cosmochimica Acta* 46:81–95.

Rubin A. E. 2015. An American on Paris: Extent of aqueous alteration of a CM chondrite and the petrography of its refractory and amoeboid olivine inclusions. *Meteoritics & Planetary Science* 50:1595–1612.

Rubin A. E., Trigo-Rodríguez J. M., Huber H., and Wasson J. T. 2007. Progressive aqueous alteration of CM carbonaceous chondrites. *Geochimica et Cosmochimica Acta* 71:2361–2382.

Rubin M., Altwegg K., Balsiger H., Bar-Nun A., Berthelier J.-J., Briois C., Calmonte U., Combi M., De Keyser J., Fiethe B., Fuselier S. A., Gasc S., Gombosi T. I., Hansen K. C., Kopp E., Korth A., Laufer D., Le Roy L., Mall U., Marty B., Mousis O., Owen T., Rème H., Sémon T., Tzou C.-Y., Waite J. H., and Wurz P. 2018. Krypton isotopes and noble gas abundances in the coma of comet 67P/Churyumov-Gerasimenko. *Science Advances* 4: eaar6297.

Sandford S. A., Bernstein M. P., and Dworkin J. P. 2001. Assessment of the interstellar processes leading to deuterium enrichment in meteoritic organics. *Meteoritics & Planetary Science* 36:1117–1133.

Scott E. R. and Krot A. N. 2005. Chondritic meteorites and the high-temperature nebular origins of their components. In *Chondrites and the protoplanetary disk*, vol. 341, edited by Krot A. N., Scott E. R. D., and Reipurth B. San Francisco: Astronomical Society of the Pacific. p. 15.

Vacher L. G., Marrocchi Y., Verdier-Paoletti M. J., Villeneuve J., and Gounelle M. 2016. Inward radial mixing of interstellar water ices in the solar protoplanetary disk. *The Astrophysical Journal Letters* 827:L1.

Vacher L. G., Marrocchi Y., Verdier-Paoletti M. J., Villeneuve J., and Gounelle M. 2017. Erratum: "Inward Radial Mixing of Interstellar Water Ices in the Solar Protoplanetary Disk"(2016. ApJL. 827. L1). *The Astrophysical Journal Letters* 836:L16.

Vinogradoff V., Le Guillou C., Bernard S., Binet L., Cartigny P., Brearley A. J., and Remusat L. 2017. Paris vs. Murchison: Impact of hydrothermal alteration on organic matter in CM chondrites. *Geochimica et Cosmochimica Acta* 212:234–252.

Vinogradoff V., Bernard S., Le Guillou C., and Remusat L. 2018. Evolution of interstellar organic compounds under asteroidal hydrothermal conditions. *Icarus* 305:358–370.

Weimer D., Busemann H., Alexander C. M., and Maden C. 2017. The effect of aqueous alteration on primordial noble gases in CM chondrites. *80th Annual Meeting of the Meteoritical Society*.

SUPPORTING INFORMATION

Additional supporting information may be found in the online version of this article:

Fig. S1: A) Scanning electron microscopy (SEM) images of CM 2.9 (fragment 5) and CM 2.7 (taken close to fragment 8) areas of our thin section of the Paris meteorite. The more altered zones are marked by the presence of carbonates and phyllosilicates in the matrix. These minerals are absent from the pristine areas, where free Fe-Ni metal is observed. B) Enlarged view of the two faces of our thin section of the Paris meteorite, showing the altered CM 2.7 (in blue) and the fresh CM 2.9 (in white) areas, respectively. The two yellow dotted lines show the diamond wire saw cut lines. The approximate contour lines of the four fragments (4 and 5 being CM 2.9 and 2 and 8 being CM 2.7) analyzed in this study for their heavy noble gas isotopes.

Fig. S2: ^{20}Ne, ^{36}Ar, ^{84}Kr, and ^{132}Xe pattern of release from the IOM of the Paris meteorite upon stepwise heating. Temperatures are given on the *x*-axis. The major ^{132}Xe release (>85%) occurs at 1225°C. Corresponding data are given in Tables 1, 2, 4, and 6. Uncertainties are 2σ.

Fig. S3: $^{131–136}Xe/^{130}Xe$ isotopic composition of the Paris meteorite normalized to Q-Xe (Busemann et al. 2000) (the results of the present study for the CM 2.7 and CM 2.9 bulk fragments correspond to the data points). Fission spectra for ^{238}U (left panel, dotted lines) and ^{244}Pu (right panel, dashed lines) (Porcelli and Ballentine 2002), calculated assuming that all of the excess ^{136}Xe is fissiogenic in origin, are shown for comparison. For both U and Pu, the fission spectra are within error of the data points, indicating that no distinction could be made between the major sources of fissiogenic Xe. Uncertainties are 2σ.

Fig. S4: $^{136}Xe/^{130}Xe$ measured from the four bulk fragments of the Paris meteorite (this study, in gray), normalized to the Q-phase composition (Busemann et al. 2000). For each fragment, the open ("corr. ch.") and closed ("corr. cc.") data points correspond to the $^{136}Xe/^{130}Xe$ corrected for ^{238}U- and ^{244}Pu-^{136}Xe contributions using initial $^{244}Pu/^{238}U$ of 0.0068 (chondritic value; Hudson et al. 1989) and 0.0122 (mean of carbonaceous chondrites; Kuroda and Myers 1991a, 1991b), respectively. The excess in $^{136}Xe/^{130}Xe$ relative to phase Q remains regardless of the initial $^{244}Pu/^{238}U$ taken. Uncertainties are 2σ.